Transport in Porous Media
https://doi.org/10.1007/s11242-018-1202-3

Microfluidics for Porous Systems: Fabrication, Microscopy and Applications

Alireza Gerami[1] · Yara Alzahid[1] · Peyman Mostaghimi[1] · Navid Kashaninejad[2] · Farzan Kazemifar[3] · Tammy Amirian[4] · Nader Mosavat[5] · Majid Ebrahimi Warkiani[2,6] · Ryan T. Armstrong[1]

Received: 29 May 2018 / Accepted: 15 November 2018

Abstract
No matter how sophisticated the structures are and on what length scale the pore sizes are, fluid displacement in porous media can be visualized, captured, mimicked and optimized using microfluidics. Visualizing transport processes is fundamental to our understanding of complex hydrogeological systems, petroleum production, medical science applications and other engineering applications. Microfluidics is an ideal tool for visual observation of flow at high temporal and spatial resolution. Experiments are typically fast, as sample volume is substantially low with the use of miniaturized devices. This review first discusses the fabrication techniques for generating microfluidics devices, experimental setups and new advances in microfluidic fabrication using three-dimensional printing, geomaterials and biomaterials. We then address multiphase transport in subsurface porous media, with an emphasis on hydrology and petroleum engineering applications in the past few decades. We also cover the application of microfluidics to study membrane systems in biomedical science and particle sorting. Lastly, we explore how synergies across different disciplines can lead to innovations in this field. A number of problems that have been resolved, topics that are under investigation and cutting-edge applications that are emerging are highlighted.

Keywords Microfluidics · Porous media · Flow visualization · On-a-chip applications · Lab-on-a-chip · Micromodels

Alireza Gerami and Yara Alzahid have contributed equally to this manuscript.

✉ Alireza Gerami
a.gerami@unsw.edu.au

1 School of Minerals and Energy Resources Engineering, University of New South Wales, Sydney, Australia

2 School of Biomedical Engineering, University Technology Sydney, Sydney, Australia

3 Department of Mechanical Engineering, California State University Sacramento, Sacramento, CA, USA

4 Australian School of Petroleum, University of Adelaide, Adelaide, Australia

5 Faculty of Engineering and Technology, Muscat University, Muscat, Oman

6 Institute of Molecular Medicine, Sechenov First Moscow State University, Moscow, Russia

Published online: 26 November 2018

1 Introduction

The flow and transport of phases and components through porous media is central to subsurface engineering applications, biological engineering technologies, energy-related research and many other disciplines. A complete understanding of the physiochemical mechanisms regarding flow and transport that occur at the length scale of micrometers is essential to the success of these technologies. In particular, the ability to manipulate fluids at the micrometer length scale is paramount. Microfluidics provides a platform to facilitate these efforts. Microfluidics deals with the study of fluids at the microscale (10^{-6}–10^{-3} m) by utilizing miniaturized devices. It is primarily used to study the science of fluid flow and transport phenomena in microstructures. The concept of microfluidic devices originated from technologies developed by the field of micro-electromechanical systems (MEMS) (Atencia and Beebe 2005; Verpoorte and De Rooij 2003). There are vast applications of microfluidics, some of which include drug screening, biomedical analyses, genetics, proteomics and energy conversion (Kjeang et al. 2009; Sinton 2014). Advantages of microfluidics include: small sample and reagent volumes, high-resolution analysis and small footprint for analytical devices (Davies et al. 2015; Trietsch et al. 2011; Whitesides 2006a). Interest in microfluidics is dated since the late 1950s, and in the last 30 years, the numbers of publications on microfluidics have rapidly increased, reaching a total of approximately 6650 journal articles since 1991 (obtained from a refined search in Google Scholar). Nowadays, advanced fabrication methods, experimental setups and applications are continuously evolving and will continue into the unforeseeable future.

This review highlights microfluidic fabrication techniques and focuses on recent advances, such as geomaterial and membrane-based microfluidics. We also cover common visualization methods and experimental setups and emphasize different microscopic techniques that are currently available. We then discuss recent innovations relevant to porous media research across different disciplines, such as petroleum engineering and environmental engineering with a focus on hydrocarbon recovery and CO_2 sequestration, and biomedical engineering in regard to cell sorting and tissue engineering. The study of microfluidics is a vast field with over 6650 journal articles since 1991. Thus, it is neither possible nor instructive to cover all of these great works. As such, we provide a more detailed review of applications from a range of different disciplines to highlight the utility of microfluidics for porous media research. This review is intended for researchers and scientists who are new to the field of microfluidics. It introduces existing fabrication and visualization options and then illustrates examples of specific applications.

2 Fabrication Techniques

Silicon has been the primary material used for fabricating microfluidics devices with well-established processing and fabrication methods for various applications. Other materials have been used to circumvent the drawbacks from using silicon, such as the high cost and opaque nature (Gravesen et al. 1993; Haeberle and Zengerle 2007; Kim et al. 2008b; McDonald et al. 2000; Whitesides 2006b). These materials include glass and polymeric materials, such as polymethylmethacrylate (PMMA), polystyrene (PS), polycarbonate (PC) and, the most commonly used material, polydimethylsiloxane (PDMS), due to its flexibility in molding, optical transparency and biocompatibility (Lei 2015). Depending on the material being used, one of two primary methods is used to generate a microfluidics device: photolithography or

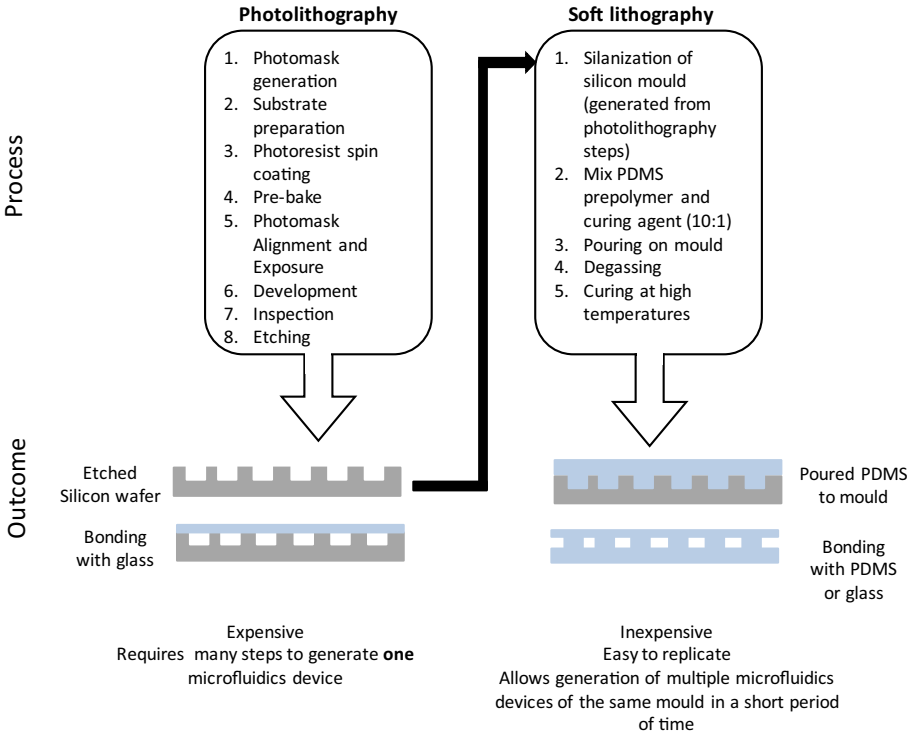

Fig. 1 Comparison of photolithography and soft lithography techniques. Photolithography undergoes many steps in order to create one microfluidics device, whereas soft lithography uses a master mold created by photolithographic methods

soft lithology, as summarized in Fig. 1. With photolithography, the microfluidic pattern is etched into a solid substrate, typically, silicon-based devices, while for soft lithology, which is used for PDMS devices, a negative mold is created in which a liquid agent is poured and then cured.

2.1 Silicon-, Glass- and Polymer-Based Microfluidics

Microfabrication using silicon as the substrate includes the following processes: photolithography, thin-film deposition, etching and bonding. Photolithography results in the transfer of a pattern from a photomask to a silicon wafer, or substrate, that is initially coated with a light-sensitive material called photoresist. This process is performed by employing ultraviolet (UV) light, the details of which are provided in Berkowski et al. (2005); Stevenson and Gundlach (1986). In order to achieve nanometer features on the photoresist, electron beam lithography (EBL) can be used (Chen 2015). Thin-film deposition refers to a process of adding thin films, such as silicon dioxide, polysilicon, silicon nitride and metal onto the surface of a silicon wafer. Physical vapor deposition (PVD) and chemical vapor deposition (CVD) are two techniques used for thin-film deposition; however, PVD is most commonly used. PVD uses a condensable vapor of the desired material to deposit a thin film onto a substrate through a vacuum or low-pressure gaseous environment. Etching of the substrate can

be performed with wet etching (using chemical solutions) and dry etching (plasma) methods. Choosing which type of etching to use for a microfabrication process depends highly on the structures being etched, type of silicon wafer used and the aspect ratio of the channels that are to be etched. In wet etching, isotropic and anisotropic etching can be achieved, which refers to equal or unequal etching rate in all directions, respectively (Franssila 2010; Madou 2002). As for dry etching methods, it includes reactive ion etching (RIE) and deep reactive ion etching (DRIE). The detailed mechanism of etching can be found in Laerme et al. (1999), Schwartz and Schaible (1979) and Wu et al. (2010). Lastly, to create an enclosed microfluidic device, the substrate is bounded to a cover. The type of bonding technique employed depends on the material being bonded to silicon. For instance, silicon-to-silicon bonding can be achieved via fusion bonding; however, silicon-to-glass bonding can be achieved via anodic bonding techniques (Iliescu et al. 2012; Lu et al. 2008; Schmidt 1998; Tsao and DeVoe 2009).

Glass is another material that can be used in combination with silicon, or as an alternative material, which can allow for direct visualization to the fluids in the microfluidics device. The most common glass used is borosilicate glass (Albaugh 1991; Lei 2015). Borosilicate glass has a similar thermal expansion coefficient to that of silicon, resulting in low residual stress after bonding. Also, the chemical composition of borosilicate glass helps the bonding process (Albaugh 1991). Similar to silicon, glass goes through photolithographic steps and can be patterned by wet or dry etching techniques or laser ablation. Glass can bond to silicon through anodic bonding, PDMS through plasma treatment or itself by thermal bonding (Silverio and de Freitas 2018).

For polymer-based microfluidic devices, soft lithography is commonly used, which is based on replica molding for micro- and nanofabrication (Kalkandjiev et al. 2010; Karadimitriou and Hassanizadeh 2012; Kim et al. 2008b; Stephan et al. 2007). Photolithography is first used to generate the so-called master mold, typically on a silicon wafer. This is a negative image of the desired pattern to be created. The master silicon wafer is then silanized, typically using trichlorosilane ($HSiCl_3$) to create a hydrophobic surface on the master mold for successful PDMS coating. PDMS is then prepared by mixing PDMS monomer and curing agent. By pouring the PDMS mixture into the master mold, followed by degassing in a vacuum chamber, and curing, the channel structures are fabricated. The pattern is then peeled from the master mold and sealed to a substrate, typically glass or PDMS, by various methods, such as plasma treatment (Brian and Ellis 2016; Friend and Yeo 2010; Jahanshahi et al. 2013; Li et al. 2013; Nan et al. 2015; Shiu et al. 2008; Tan et al. 2010; Wong and Ho 2009; Yaozhong et al. 2014). Other bonding methods are discussed in Karadimitriou et al. (2013). The main advantage of using soft lithography is rapid prototyping and requires less equipment, which translates into less expense associated with this type of lithography (Anbari et al. 2018). Although creating the master silicon mold can be expensive, creating several PDMS devices from that master mold makes this option cost-efficient. Hence, PDMS-based microfluidic devices are continuously utilized, customized and developed. For instance, Zarikos et al. (2018) integrated fiber optic pressure sensors into a PDMS micromodel to measure pore pressure under specific transient two-phase flow conditions, Karadimitriou et al. (2013) developed a procedure for making uniformly and stably hydrophobic PDMS micromodels, and Gerami et al. (2018) fabricated a dual-wettability PDMS device for studying flow in regions with different wettabilities. Similar to PDMS, PMMA is another transparent thermoplastic polymer (i.e., hardens at high temperatures) that is used for microfluidic purposes. PS and PC are also other thermoplastic polymers that have gained interest in cell culture microfluidics, due to their hydrophilic nature and biocompatibility (Lei 2015). Hot embossing, microinjection molding (μIM) and micromilling are the most commonly used techniques to create microstructures from PS or PC (Giboz et al. 2007; Guckenberger et al. 2015).

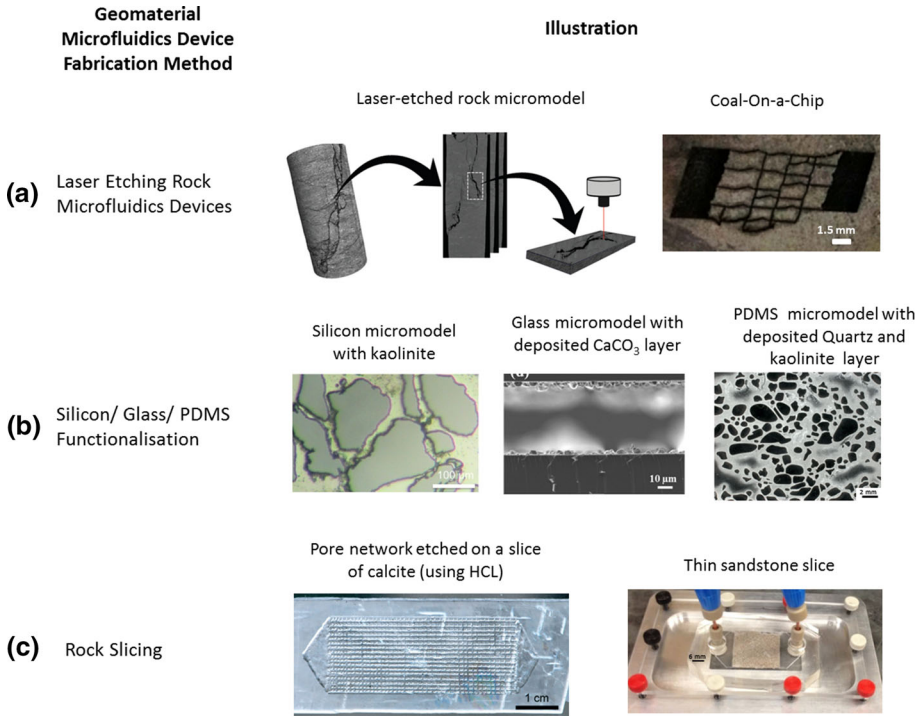

Fig. 2 Overview of geomaterial microfluidics device fabrication methods. **a** Laser etching on real rock surfaces. Reproduced with permission from Gerami et al. (2017) and Porter et al. (2015a). **b** Silicon/glass/PDMS functionalization by attaching relevant rock minerals. Reproduced with permission from Song and Kovscek (2015) and Wang et al. (2017). **c** Rock slicing. Reproduced with permission from Song et al. (2014) and Singh et al. (2017). Images are representatives of each technique

2.2 Geomaterial Microfluidics

Fabrication of geomaterial microfluidics has received attention in the fields of hydrology and petroleum engineering, in which pore-scale flow and/or transport is often dictated by surface chemistry (Bowden et al. 2016; Gerami et al. 2017; Mahoney et al. 2015, 2017; Morais et al. 2016; Oh et al. 2017; Porter et al. 2015b; Song et al. 2014; Tanino et al. 2018; Wang et al. 2017; Zhang et al. 2018). In Fig. 2, we provide an overview of the different geomaterial microfluidics chips that have been reported in the literature.

A laser-etched rock substrate was first employed by Porter et al. (2015b) in microfluidic experiments to provide a tool for more realistic and comprehensive flow visualization. Geomaterial chips have the advantage of mimicking the chemical and physical properties of natural porous media. This is of importance, particularly for unconventional reservoirs, due to their heterogeneity, unique fracture system and specific mechanisms such as swelling and shrinkage, which affects flow and transport (Britt and Schoeffler 2009; Liu et al. 2017). Gerami et al. (2017) used an image of a coal fracture obtained from micro-computed tomography (micro-CT) for fabrication of a coal geomaterial microfluidic chip. The fracture pattern was imported to a CAD drawing, which was then etched on a flat coal surface using the laser machine microSTRUCT-C (3DMicromac, Chemnitz, Germany).

Song et al. (2014) developed a method to etch microchannels into calcite rock. This method includes firstly cutting a calcite crystal into 3-mm-thick wafers and secondly dipping the calcite wafer into molten beeswax heated to 150 °C and left to solidify. The desired microfluidics patterns were then etched via laser into the wax, and lastly, the wax and calcite were immersed in hydrochloric acid, resulting in the inscription of the microfluidics channels into the calcite crystal. This process allowed for the study of acid injection and dissolution in natural calcite rock, which can provide insights into pore-level geochemistry. Wang et al. (2017) used a simple glass micromodel, which was composed of a simple channel, and coated a layer of $CaCO_3$ nanocrystal. The purpose of their study is to create a realistic representation of carbonate rock. This was achieved by first functionalizing the inner wall of the microfluidic channel by adding a silane agent and then adding Ca^{2+} and $CO3^{2-}$ ions to attach to the multiple COO^{-} sites, resulting in a uniform thickness of $CaCO_3$ nanocrystal layer on the inner surface of the microfluidic silica channels. Scanning electron microscopy (SEM) imaging, energy-dispersive X-ray spectroscopy (EDS) and Raman spectroscopy were performed to visualize the presence of $CaCO_3$ nanocrystals.

Song and Kovscek (2015) developed a functionalized silicon microfluidic device coated with clay minerals, mimicking a sandstone pore surfaces. This approach allows pore-scale visualization of fluid–solid interactions in a sandstone pore geometry. The authors used this design to analyze the effect of low-salinity brine injection to the detachment of clay (Song and Kovscek 2016). Singh et al. (2017) designed a microfluidic platform called the real rock-microfluidic flow cell (RRMFC). This approach involves mounting a 500-μm sandstone rock section between two PDMS covers. The authors investigated the mineralogy and geochemistry of the microfluidic platform using several microscopic approaches, such as transmitted, cathodoluminescence (CL) and confocal laser microscopy.

Other than glass functionalization, work has been done to functionalize PDMS microfluidics devices (Alzahid et al. 2018; Zhang et al. 2018). Zhang et al. (2018) introduce the concept of layer-by-layer (LbL) coating of PDMS microfluidics devices. Their LbL process requires subjecting PDMS to plasma, followed by injection of poly(diallyldimethylammonium chloride) (PDDA) solution and clay suspension alternately. DI water is injected between the two steps (PDDA and clay suspension injection) to remove any loose particles, in addition to drying the microfluidic device in each step. This cycle is repeated 2–3 times to get the desired minerals thickness. Alzahid et al. (2018) developed another approach to functionalizing PDMS and used two different rock minerals to obtain sandstone and carbonate microfluidic devices. Their method involved plasma treating PDMS, followed by injection of minerals solution, and the PDMS containing the minerals was then dried, cleaned and subjected to another plasma treatment to bond it to the PDMS cover. Finally, polyvinyl alcohol (PVA) was injected immediately after the second plasma treatment to make the PDMS geomaterial microfluidic device water wet. As mentioned previously, these geomaterial approaches are novel tools to capture rock–fluid subsurface phenomena, such as snap-off, wettability and dissolution. Figure 3 shows a schematic illustration of the two PDMS functionalization methods.

2.3 Membrane-Based Microfluidics

For biomedical research, the attachment of cells to surfaces depends on two important factors: the chemistry and physical structure of the microfluidic device. For organ-on-a-chip devices, a semipermeable porous membrane is sandwiched between upper and lower channels. Epithelial cells (e.g., lung, liver) are cultured on the top side of the membrane, while

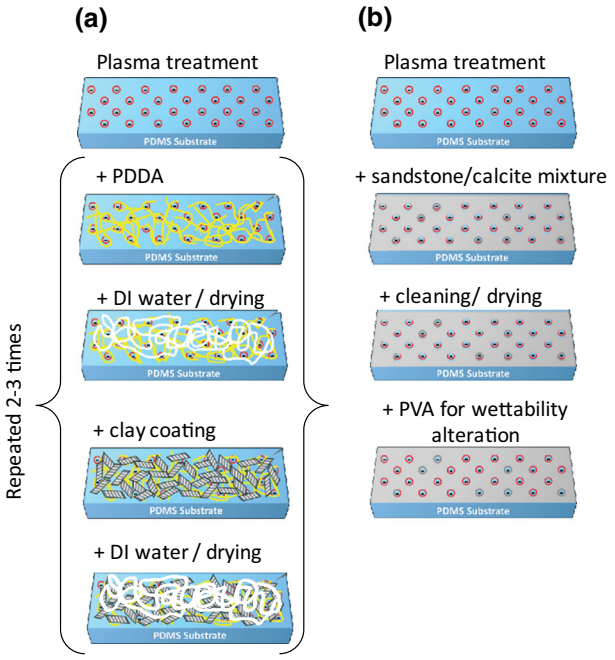

Fig. 3 Proposed methods of PDMS functionalization. **a** Explains the process of layer-by-layer, reproduced from Zhang et al. (2018). The yellow and white lines indicate PDDA and water, respectively. Clay is indicated as the irregular shapes in black dashed lines. Reproduced with permission from (Zhang et al. 2018). **b** Explains the functionalization method proposed by Alzahid et al. (2018). The gray color indicates the sandstone or the calcite mixture attached to the PDMS

endothelial cells (which represent blood capillaries) are cultured on the other side. The culture medium flows from the lower channel, and air passes through the epithelial cells from the upper channel. Accordingly, the nutrients and waste materials are exchanged using a porous membrane, and physicochemical signaling between tissues is facilitated in a shear-free co-culture environment. Figure 4 represents a typical microfluidic device for organ-on-a-chip.

To better recapitulate physicochemical properties and provide a microenvironment, similar to in vivo conditions, the incorporation of a micro-/nanoporous membrane in these organ-on-a-chip devices is essential. To become a suitable for organ-on-a-chip platform, the porous membrane needs to entail several characteristics. First, the membrane should be biocompatible and have properties similar to those of the native extracellular matrix (ECM). Second, the membrane should be thin enough to allow rapid mass transport and the size of the pores should be controlled systematically. Finally, the membrane should be mechanically robust and optically transparent for in situ or off-chip analysis. For a conventional migration assay, the commercially available polyester and polycarbonate membranes are widely used. For most organ-on-a-chip platforms, polymer membranes mainly fabricated from (PDMS) are utilized, which provides complete optical access, secure sealing and strong bonding. However, these synthetic PDMS membranes have several disadvantages. First, the fabrication for such membranes is relatively time-consuming and expensive. Second, since the surfaces of these PDMS membranes are totally flat, after cell seeding inside the microfluidic device, the cells grow in a two-dimensional (2D) monolayer structure. Although the cells are in a

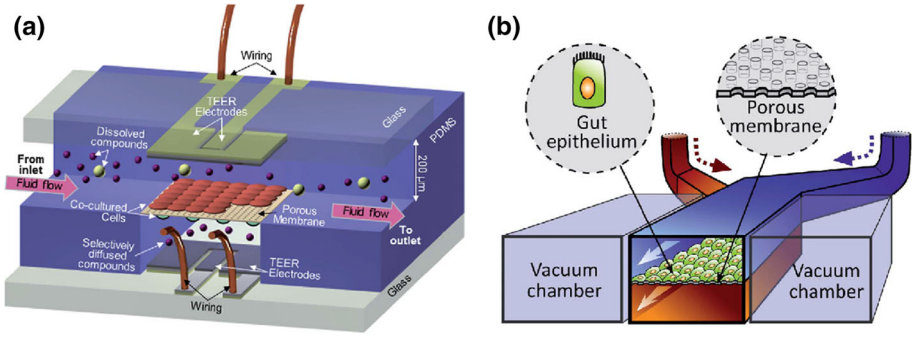

Fig. 4 Schematic representation of the application of membrane-based microfluidic devices in organ-on-a-chip platforms. **a** Various components of blood–brain barrier-on-a-chip with embedded electrodes trans-endothelial electrical resistance. Reproduced with permission from Booth and Kim (2012). **b** Gut-on-a-chip platform with porous PDMS membrane which allowed compartmentalization of the system coated with ECM and seeded by human gut epithelial cells. Reproduced with permission from Kim et al. (2012b). The PDMS membrane is irreversibly bound to the top PDMS microchannel using plasma treatment. To facilitate the bonding, the PDMS membrane and the microchannel are heated at 80 °C overnight. Before plasma bonding these components to the lower PDMS channel, some parts of the membrane are torn using forceps to generate the hollow structures acting as vacuum channels. The vacuum channels could mimic the movement of small intestine by applying the cyclic suction

dynamic and perfusion microbioreactor, 2D monolayer cell culture cannot indeed recapitulate in vivo cell signaling.

Considering the aforementioned limitations of polymer membranes, nanofibrous membrane fabricated using electrospinning (Ahmed et al. 2015) can be considered a better candidate for applications in cell culture and tissue engineering (Wang et al. 2013a; Moghadas et al. 2017a). This technique has been used to fabricate a cost-effective and robust scaffold for three-dimensional (3D) cell cultures (Moghadas et al. 2017a). As shown in Fig. 4a, b, by increasing the PDMS mass ratio during electrospinning, the porosity and hydrophobicity of the membrane can be controlled (Moghadas et al. 2017a). Seeded epithelial lung cancer cells were aggregated into 3D multicellular spheroids on such electrospun membranes (Moghadas et al. 2017a). The only limitation of using these nanofibrous electrospun membranes is their opacity. The non-transparent properties of the electrospun membrane make further analysis with bright-field microscopy difficult. Nanofilm-based membranes fabricated by various nanofabrication techniques, such as layer-by-layer assembly (Jiang and Tsukruk 2006), are also an attractive alternative for the microfluidic organ-on-a-chip application. Using a transparent and biocompatible polymer, poly(lactic acid) (PLLA) nanofilms, Pensabene et al. (2016) fabricated a dynamic microfluidic cell culture platform by embedding PLLA ultrathin membrane inside the device, as shown in Figs. 4d and 5c (Pensabene et al. 2016). In addition, the reproducibility limitations and fragile nature of such an ultrathin membrane may affect its widespread use.

3 Visualizations and Measurements

A basic microfluidic setup consists of a pump, microfluidic device, pressure controllers and visualization system. The fluid is injected into the chip pattern through the inlet tube where it displaces/interacts with resident fluid. By utilizing syringe pumps, high-pressure

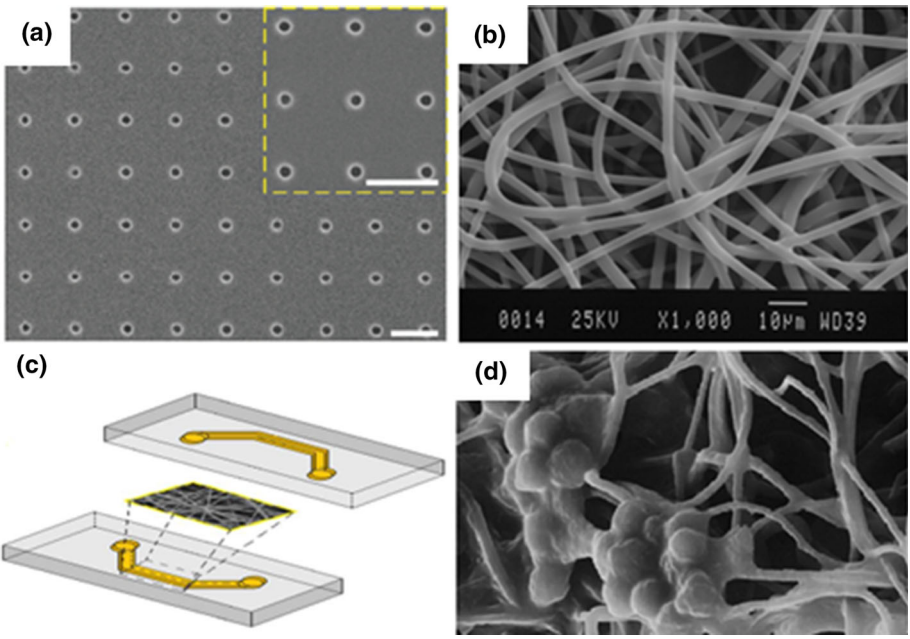

Fig. 5 Characterization of porous membrane used for cell culture applications. **a** Scanning electron microscopy (SEM) free-standing PDMS through-hole membrane. Such membrane is smooth. The scale bars are 5 μm. Reproduced with permission from Le-The et al. (2018). **b** SEM image of PDMS electrospun membrane. Reproduced with permission from Moghadas et al. (2017a). Unlike the smooth PDMS membrane, the electrospun membrane has 3D structures. **c** The electrospun membrane was imbedded between two PDMS microchannels. **d** SEM images of human lung cancer epithelial cells cultured on the electrospun membrane integrated into the microchip. Due to the 3D structure of the membrane, the cells are formed in a 3D cluster. Reproduced with permission from Moghadas et al. (2018)

pumps, pressure transducers, flow sensors, pressure cells, heaters, etc., the setup can be modified for specific applications (Karadimitriou and Hassanizadeh 2012). Overall, the real-time visualization, quantification and/or control of flow and/or transport in the micromodel are considered a significant advantage of microfluidic studies and applications. In particular, the visualization method is critical for a successful microfluidic experiment and can be used as both a qualitative and quantitative tool. For instance, relative permeability data of water and gas flow in coal fractures are measured based on the images obtained from the microfluidic experiments (Gerami et al. 2016) (Fig. 6a). 3D observation of a non-dyed buffer displacing a fluorescein-dyed buffer (Fig. 6c) (Singh et al. 2017) and the transport of decane (Fig. 6b) and dyed CO_2 (Fig. 6d) (Kazemifar et al. 2015) are other examples of visualizations obtained by microfluidic experiments.

3.1 Transmitted and Reflected Microscopy

A camera coupled to a microscope is commonly employed for the visualization of microfluidic experiments (Gunda et al. 2011; Rangel-German and Kovscek 2006; Xu et al. 2014). This setup is effective for focusing on a specific area in the micromodel at high resolution (>1 μm) and for the measurement of parameters, such as contact angle and interfacial curvature (Karadimitriou and Hassanizadeh 2012). In addition, high-speed cameras can be

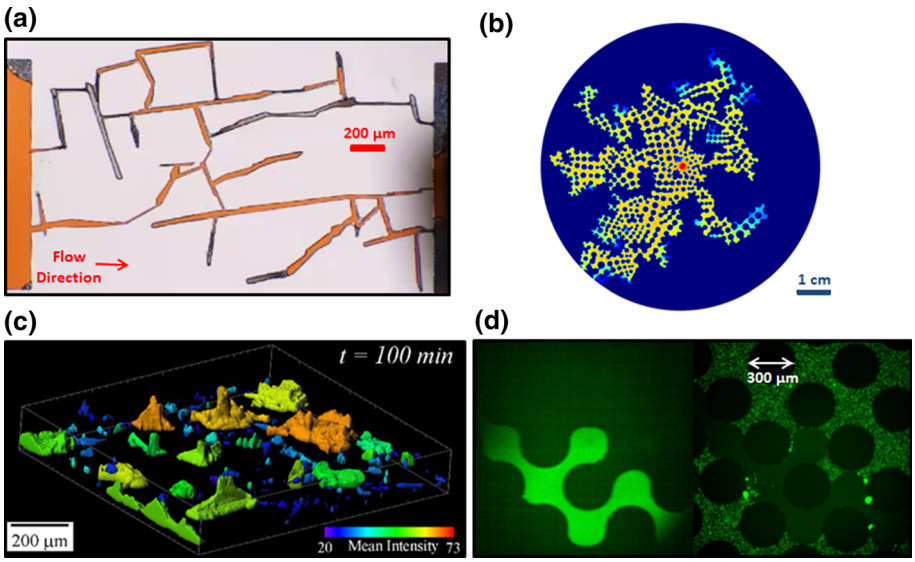

Fig. 6 **a** Dyed colored fluid displacing gas within coal fractures. Transmitted microscopy is utilized to visualize the flow transport. Reproduced with permission from Gerami et al. (2016). **b** Direct visualization is employed to observe the displacement of decane oil in a random pore network model developed by PDE tool in MATLAB. The injection starts from the center of the circle. **c** Confocal laser microscope is utilized to observe the displacement of fluorescein-dyed buffer by a non-dyed buffer at 100 min after the injection. Reproduced with permission from Singh et al. (2017). **d** Sample images of dyed CO_2 (left) and tracer particle image (right) in a silicon-based micromodel using a dual-camera imaging setup. Reproduced with permission from Kazemifar et al. (2015)

incorporated to study rapid events (Armstrong and Berg 2013; Moebius and Or 2012, 2014). For microfluidic chips with one opaque side, the light source and the optical access have to be on the same side of the chip (such as reflected microscopes). For transparent porous media, either a transmitted microscope (light source and optical access are at the opposite side of the chip) or a reflected microscope can be employed.

A setup of camera(s) without a standard microscope is utilized for experiments that require a larger field of view (e.g., flow visualization over time) or for experiments with high acquisition rates (Alzahid et al. 2017; Hematpour et al. 2011; Moebius and Or 2012). With these setups, cameras are placed at flexible distances from the micromodel at any suitable orientation, to capture images and videos from the flow. Because no microscope is coupled to the camera, generally lower-resolution images are obtained for the given camera objective. Karadimitriou et al. (2012) built a customized setup by utilizing a prism between the light source and the objective lens. A beam-splitter box was utilized to produce identical images of the micromodel sections in different directions, and cameras were placed around the box to visualize all of the projected images. Hence, they could capture high spatial and temporal resolutions of the entire micromodel. This setup was utilized for studying flow in elongated micromodels (Karadimitriou et al. 2014) and was then extended to reflected microscopy following the same visualization principles (Godinez-Brizuela et al. 2017). In other setups, a long-distance microscope objective is employed to focus the emitted light from the flow, onto the detector of a camera. This allows for relatively low magnification (~3×, translating to ~2 µm/pixel) and a sufficient field of view (8.8 mm × 5.5 mm) to cover the entire microfluidic chip as employed for the fluorescence imaging setup in Chen et al. (2017) and

Fakhari et al. (2018). Although a conventional epifluorescence microscope can accommodate a low-magnification objective, the large working space of a long-distance microscope provides additional flexibility and space for setting up the experiment.

3.2 Confocal Microscopy

Confocal microscopy is used for three-dimensional (3D) imaging and for microfluidic experiments with high-resolution requirements (<1 μm). This setup can observe relatively slow displacements that occur over a length scale less than the optical diffraction limit (Karadimitriou and Hassanizadeh 2012). This setup can also provide images over the depth of the chip up to a total depth of around 250 μm. For instance, Zhang et al. (2013) utilized confocal microscopy to monitor colloids transport during two-phase flow in a microfluidic device. Datta et al. (2013) captured the single-phase flow in a 3D packed glass bead porous model via a confocal laser scanning microscope, and in a subsequent publication, they analyzed two-phase fluid flow using the same method in a porous medium (Datta et al. 2014). Zevi et al. (2005) utilized this visualization technique to measure water meniscus shape and water film thickness on sand grains in an unsaturated horizontal chamber. In addition, numerous researchers have used confocal laser scanning microscopy (CLSM) to visualize the growth of biofilms in microfluidics devices. They studied bacteria producing a green fluorescent protein, and different fluorescent staining procedures are utilized (Leis et al. 2005; Rodríguez and Bishop 2007). Concerning flow and transport in porous media, the prominent application of CLMS is the tracking of particles to measure local velocities.

3.3 Fluorescent Microscopy

To distinguish between fluid phases during flow, a fluid can be mixed with dye (Yadali Jamaloei and Kharrat 2009), light intensity changes can be monitored (Chapman et al. 2013), or fluorescent particles can be added to the flow (Kazemifar et al. 2016). In fluorescent visualization, the solution is tagged with a fluorescent dye, and a light source is utilized to excite the fluorescent molecules. The fluorescence signal is at a longer wavelength with respect to the incident (excitation) wavelength, commonly called the Stokes shift (Albani 2011), and a digital camera captures the long-pass-filtered light.

Fluorescence detection methods are convenient because of the simplicity and low detection limit (Kim et al. 2011; Martínez-Máñez and Sancenón 2003). The concentration of a target analyte can be measured in biosamples using this technique (Kim et al. 2011). For instance, Nolan and Lippard (2008) investigated the detection of mercury ion with sufficient selectivity. By monitoring the fluorescence intensity changes, Pb (Lead) is detected in a microfluidic channel where the surface is functionalized with a fluorophore (Basabe-Desmonts et al. 2004). By using rhodamine derivatives, chemosensors can be designed for metal ion detection (Kim et al. 2008a). Although rhodamine derivatives are non-fluorescent, the fluorescence emission is provided by the corresponding spirolactam (Yang et al. 2005). Mela et al. (2005) coated the surface of a microfluidic network with rhodamine B and utilized fluorescent microscopy techniques for local pH measurements. Chang et al. (2017) used pH-sensitive dye pHrodo® Red (Life Technologies, Carlsbad, CA), to study dissolution of CO_2 in water during a drainage process in a porous micromodel. Fluorescein is another water-soluble pH-sensitive dye whose fluorescence intensity increases with pH of the solution in the pH range of ~ 4–8 (Doughty 2010; Martin and Lindqvist 1975).

3.4 Microscopic Particle Image Velocimetry (Micro-PIV)

Particle image velocimetry (PIV) is a particle-based, nondestructive, optical diagnostic technique for fluid velocity measurement (Adrian and Westerweel 2011). In this technique, fluid is tagged with tracer particles that, when subjected to laser, can illuminate and is then imaged at two time instants separated by a set time delay, Δt. The image is subdivided into small interrogation windows (IW) that contain typically ~ 10 particles. The average displacement of particles ($\Delta\vec{x}$) in each IW can be obtained by cross-correlation analysis between the two image frames. Consequently, $\Delta\vec{x}/\Delta t$ yields the average velocity vector, $\vec{u}$, of particles in that IW. Hence, each image pair yields one velocity vector field, whose spatial resolution is determined by the size of the IW. A variant of PIV that is tailored for flow diagnostics at the microscale is microscopic particle image velocimetry (micro-PIV) (Meinhart et al. 1999; Santiago et al. 1998). Numerous factors must be considered to produce reasonable velocity measurements. These factors include: illumination method, tracer particle density and size, camera sensor versus particle diameter and chemical interactions.

Due to geometrical limitation, it is not possible to generate a light sheet in microfluidic applications (as is customary in standard PIV); thus, volume illumination is employed where particles in the entire depth of the microfluidic device are illuminated. Consequently, out-of-focus particles take part in the cross-correlation function that is used to determine average particle displacement in an IW (Olsen and Adrian 2000). Moreover, to suppress the background scattered light and increase the signal-to-noise ratio in PIV images, fluorescent particles are used, allowing long-pass filtering of the scattered light. The ideal illumination source for PIV application is a pulsed laser that delivers an intense pulse of energy over a very short period of time (for instance, ~ 10 ns for Nd:YAG lasers). The short pulse of the laser ensures that the particles are frozen in the image, and no streaking occurs from the movement of particles during exposure. The particles dispersed in the fluid phase(s) acting as tracers must have specific properties to faithfully follow the fluid flow. First, the particles' density should (nearly) match that of the fluid to eliminate gravity/buoyancy driven motion. Also, for particles to follow rapid flow acceleration and/or decelerations, the Stokes number, which represents the tracer particle typical response time to flow, should be very small (Kazemifar et al. 2015). Moreover, the particle diameter must be 10^1–10^2 times smaller than the smallest channel dimension to avoid blocking effects. However, with small particles, displacement of the tracer particles due to Brownian motion must be considered (Santiago et al. 1998). Other sources of error in determining average displacement of particles from the cross-correlation function pertain to the particle image diameter and resolution of the camera sensor (Christensen 2004; Westerweel 1997). Lastly, the material of the tracer particle should be considered, which is typically a polymer. Thus, depending on the fluids, the physical and chemical compatibility of the polymer must be considered. This is particularly important in studies with supercritical CO_2 (Kazemifar et al. 2015), which is a strong solvent and can cause polymer swelling (Hilic et al. 2001; Rindfleisch et al. 1996; Sato et al. 1999; Webb and Teja 1999). Further details on the theory and practice of this technique are provided in (Adrian and Westerweel 2011), Raffel et al. (2013) and Tropea et al. (2007).

3.5 Raman Spectroscopy

Raman spectroscopy detects molecule-specific information at the microscale by measuring the vibrational modes of molecules (Chrimes et al. 2013). Details on Raman spectroscopy are explained in Chrimes et al. (2013). Raman coupled with microfluidic experiments could

provide information on miscible and immiscible fluids, such as identifying chemical pathways and structures, understanding intrinsic kinetics and thermodynamics and improving the accuracy of mass transport coefficients. Several studies have utilized Raman spectroscopy with microfluidic devices. For instance, Raman spectroscopy can be used to validate the presence of relevant rock minerals on geomaterial microfluidic devices (Lee Seung et al. 2016; Wang et al. 2017). In addition, Raman was also used to study the polymorphs of calcite during precipitation caused by acid (Singh et al. 2015; Yoon et al. 2012), which is one of the fundamental processes in subsurface engineering. Others have used Raman spectroscopy to study the CO_2 solubility in water and brine (Guo et al. 2014, 2015; Liu et al. 2012; Lu et al. 2013; Morais et al. 2015). The Raman spectra obtained from microscopic imaging provide a small cross section of the sample. This is because the light spot for each pixel (generally $0.3 \times 0.3\ \mu m^2$), which refers to the number of molecules in the spot, is also small. This is considered as one of the drawbacks of Raman spectroscopy. Kawata et al. (2017) and Deckert et al. (2015) discuss more about Raman spectra resolution and how to overcome the challenges associated with Raman spectroscopy.

4 Applications of Microfluidics

Using microfluidics for visualizing flow and transport in porous media is relevant to several engineering applications, particularly in energy-related applications (such as hydrocarbon recovery processes), and geological CO_2 sequestration. Here, the focus is on understanding a specific mechanism(s) and/or the generation of data to provide spatial and temporal concentrations/velocities used for validating numerical codes. Microfluidics is also relevant in biomedical fields, such as tissue engineering and cell sorting to engineer a specific application by controlling a particular process and/or generating a particular environment necessary for tissue development. The following subsections discuss recent advancements and applications of microfluidics within these fields.

4.1 Hydrocarbon Recovery

Enhanced oil recovery (EOR) is a broad range of processes that aims to improve oil recovery (Alagorni et al. 2015; Lake 2014). EOR processes ultimately deal with the flow and transport of chemical species and the resulting phase behavior in porous media. Microfluidic devices can serve as a good platform for assessing pore-scale chemical or thermal recovery processes. These devices can be adjusted to accommodate a testing reservoir fluid at reservoir conditions. In this section, we summarize a few selected studies that have used microfluidics for investigating EOR methods.

Low-salinity water (LSW) flooding denotes injection of diluted brine concentrations to increase oil recovery. Morin et al. (2016) introduced a novel microfluidic device to assess the effects of chemically mediated interfacial properties between oil and brine upon snap-off at the pore level. The microfluidic device formed oil drops through extensional flows and allowed the aging of crude oil against brines of different salinities, hence assessing the role of salinity in snap-off, i.e., oil droplet formation. Low-salinity brine was found to result in the preferential development of dynamic interfacial viscoelasticity, thereby suppressing pore-level snap-off events. Bartels et al. (2016) and Bartels et al. (2017) used clay-coated micromodels to investigate the low-salinity effect and its dependence on crude oil properties, presence of clay particles and aging. Amirian et al. (2017) utilized the approach, proposed

by Song and Kovscek (2015) to deposit clay particles into micromodels and visualized the micro-mechanism of displacement under LSW injection.

The effect of surfactant additives was also studied using microfluidics (Alzahid et al. 2019; de Haas et al. 2013; He et al. 2015, 2017; Nguyen et al. 2015). Yadali Jamaloei and Kharrat (2009) utilized a low-concentration surfactant solution in both water- and oil-wet glass micromodels. Different events were observed in the two micromodels. Oil-wet micromodels showed water-in-oil emulsions, which is not preferable for EOR. Water-wet micromodels displayed bridging between pores, and deformation of the residual oil, which is favorable in EOR processes. Pei et al. (2013) visualized the displacement mechanism of emulsions created from alkaline flooding (Fig. 7b). Dong et al. (2012) also conducted a microfluidic approach to studying the displacement mechanism of alkaline flooding in heavy oil. In their study, two events were observed: (1) in situ water-in-oil emulsion formation and partial change in wettability and (2) oil-in-water emulsion occurred only when adding a surfactant solution, which resulted in the mixing of heavy oil in the water phase. Unsal et al. (2016) studied the dynamic formation of micro-emulsion in situ by co-injecting decane and surfactant solution (at a specific concentration) into a T-junction capillary geometry at different salinities and flow rates (Fig. 7a). They utilized Nile Red, a unique solvatochromic dye, which allowed the micro-emulsion formation to be visualized using fluorescent microscopy. Lastly, Sedaghat et al. (2016) used several glass-etched micromodels with different fracture arrangements. They investigated the effect of fracture characteristics (length, orientation and quantity of fractures) and ASP slug compositions on heavy oil recovery.

Thermal EOR mechanisms, such as steam-assisted gravity drainage (SAGD), are mainly employed for heavy oil recovery. Conventional SAGD and hybrid SAGD processes (pentane and hexane additives) were thoroughly investigated by researchers using glass micromodel (Mohammadzadeh and Chatzis 2016; Mohammadzadeh et al. 2010). Their visualization led to in-depth understanding of micro-pore flow, and residual oil trapping mechanisms in SAGD, including (i) layered drainage flow perpendicular to the nominal oil–gaseous mixture interface and (ii) occurrence of both water-in-oil and solvent-in-water emulsions at the interface. Other pore-scale phenomena have also been observed, such as entrapment of steam and condensation, and liquid film snap-off. Sinton's laboratory introduced a microfluidic network that represented a realistic model of a typical SAGD, which was saturated with bitumen and the relevant reservoir conditions and pore sizes (de Haas et al. 2013). They achieved high-resolution visualization by using the ability of native bitumen to fluoresce in order to assess the alkaline additive (Fig. 7c). The additive significantly reduced the size of oil-in-water emulsions, and the corresponding recovery was improved by ~ 50% during SAGD. As a further step for alkaline additive screening, infrared and optical pore-scale imaging of the SAGD process using different alkaline additives were analyzed using the same micromodel (Syed et al. 2016). Using a combination of microscale flow and high-resolution temperature analysis can provide valuable insights into pore-scale phenomena, specifically the interrelationships between temperature drop at the steam chamber interface, drainage modes and recovery during SAGD. In another attempt, alcohol- and alkaline-based elements as evolving additives to improve the performance of SAGD were tested by pore-scale visualization in order to differentiate mechanisms associated with each alcohol and alkaline additive (Kim et al. 2017). It was concluded that although alcohol slightly improved the growth of steam, whereas a 10% expansion of steam was achieved by alkaline and improved recovery.

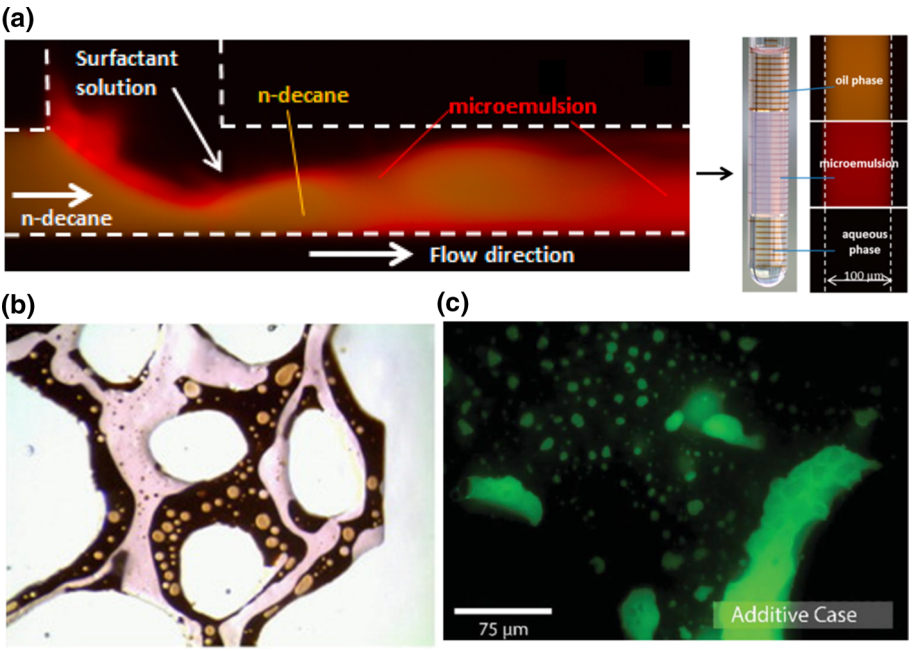

Fig. 7 The formation of emulsion systems. **a** Top view of a *T*-junction during the co-injection of surfactant solution and colored decane under fluorescent light, highlighting the micro-emulsion formation at optimum salinity during continuous flow. Black is an aqueous phase; red is micro-emulsion; and brown is decane. Reproduced with permission from Unsal et al. (2016). **b** With and without emulsions after alkaline flooding. Reproduced with permission from Pei et al. (2013). **c** With and without emulsions after steam-assisted gravity drainage (oil shown in green and water in black). Reproduced with permission de Haas et al. (2013)

4.2 CO_2 Sequestration

Carbon capture and sequestration (CCS) is where CO_2 is taken from the flue gas stream of large stationary greenhouse gas emitters (e.g., fossil fuel power plants) and then compressed and transported for storage in geological formations. This technology has received increased attention due to concerns about the effects of CO_2 on climate change and global warming (Haszeldine 2009; Pacala and Socolow 2004; White et al. 2003). Saline aquifers are among the most promising candidates as storage sites, in which pressurized CO_2 is injected into brine-saturated rock formations for permanent storage (Bachu 2000; Huppert and Neufeld 2014; Nordbotten et al. 2005). However, our understanding of the fate of injected CO_2 and its migration is still lacking as numerical models cannot fully capture the spatiotemporal evolution of injected CO_2 plumes. In this regard, microfluidic devices and micromodels are potent tools that can help us better understand CCS-relevant flow, transport and chemical processes at the pore scale.

At typical pressures and temperatures in a saline aquifer (80 + bar, 30 + °C), CO_2 exists as a supercritical fluid, i.e., pressure and temperature are beyond the critical point of CO_2 at 74 bar and 31 °C. Under these conditions, CO_2 and water have limited mutual solubility. As a reference, the solubility of CO_2 in deionized water at 297 K increases with pressure until it levels at approximately 2.5% by mole (6.1% by mass) beyond 7 MPa. On the other hand, the solubility of water in CO_2 at CCS-relevant pressures and temperatures is approximately one

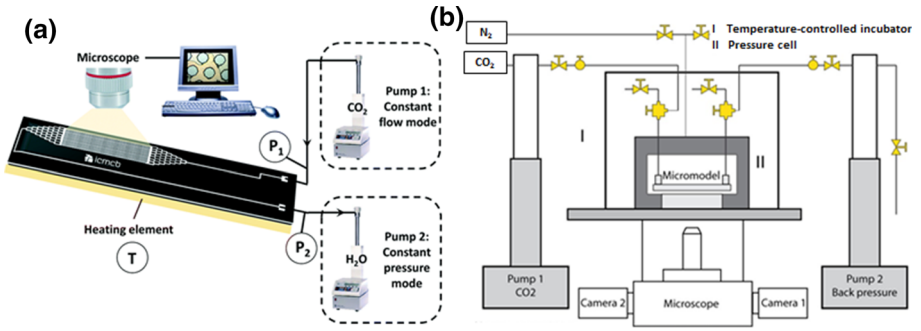

Fig. 8 Schematic of an experimental setup of a high-pressure micromodel. **a** CO_2 injection in a water-saturated pore network under identical geological conditions ($25 < T$ (°C) < 75 and $4.5 < p$ (MPa) < 8). Reproduced with permission from Morais et al. (2016). **b** Multiphase flow of liquid/supercritical CO_2 and water through a porous micromodel from below. Adapted with permission from (Kazemifar et al. 2015)

order of magnitude less than that of CO_2 in water, and it is 0.3–0.4% by mole (0.12–0.16% by mass) (Jacob and Saylor 2016; King et al. 1992; Wiebe and Gaddy 1940). In general, solubility of CO_2 in water increases with pressure and decreases with both temperature and the salinity of water/brine. Another significance of the critical point is that, in its vicinity, thermophysical properties, e.g., viscosity and diffusivity, of fluids become very sensitive to changes in pressure and temperature (Kazemifar and Kyritsis 2014). Thus, any experimental apparatus must be designed to provide precise control over pressure and temperature (Fig. 8). During injection, due to the lower viscosity of the invading CO_2 phase with respect to the resident brine phase, the advancing CO_2–water displacement front is unstable and exhibits a phenomenon referred to as *fingering*. This phenomenon can affect the displacement patterns and spatial distribution of fluid phases in a porous medium, and it has been studied extensively in the context of immiscible displacement in porous media (Homsy 1987; Lenormand et al. 1988; Zhao et al. 2016). Figure 8 illustrates experimental setups for CO_2 injection in water-saturated pore networks at reservoir condition.

For visualizing the flow in a multiphase immiscible system, such as water and liquid/supercritical CO_2, the fluorescent dye should ideally be soluble in only one of the two fluid phases. One of the few dyes satisfying this requirement is Coumarin 153 (C153), which is soluble in CO_2 but nearly insoluble in water. The emission/absorption spectra of C153 (Biswas et al. 1999; Kim et al. 2012a) and its solubility (Hae Choi et al. 1998; Shirota and Castner 2000) in CO_2 and other solvents have been documented in the literature. Numerous researchers (Chang et al. 2016; Chen et al. 2017; Fakhari et al. 2018; Kazemifar et al. 2015, 2016; Li et al. 2017; Wang et al. 2013c; Zhang et al. 2011) have used C153 to visualize liquid/supercritical CO_2 in CCS-relevant studies. Zhang et al. (2011) studied the steady-state distribution of fluid phases in a dual-permeability homogeneous micromodel during CO_2 drainage. Wang et al. (2013c) studied the steady-state distribution and displacement patterns resulting from different fingering regimes in a homogeneous micromodel during CO_2 drainage. Kazemifar et al. (2015, 2016) combined fluorescence microscopy and micro-PIV to simultaneously visualize CO_2 and record the velocity field in the aqueous phase during a drainage process in a homogeneous micromodel. They observed flow in thin water films and shear-induced recirculation in trapped water ganglia as evidenced by the motion of 1-μm tracer particles dispersed in the aqueous phase. Li et al. (2017) applied the same technique (fluorescence microscopy and micro-PIV) in a heterogeneous micromodel, using the velocity

vector field to quantify the zone of influence during Haines jump events. Fakhari et al. (2018) and Chen et al. (2017) performed coordinated lattice Boltzmann method (LBM) simulations and experiments using fluorescence high-speed imaging, to study the spatiotemporal evolution of supercritical (sc)CO_2 displacement of water in a heterogeneous micromodel. Chang et al. (2016) studied the reduction in CO_2 saturation during imbibition in a micromodel, and they calculated average mass transfer from CO_2 to the aqueous phase. Other water-soluble dyes have also been used in CCS-related studies. Zuo et al. (2013) used fluorescein and Xu et al. (2017) used rhodamine B to study depressurization-induced exsolution of CO_2 from water in micromodels. Buchgraber et al. (2012) used a general-purpose UV dye to study residual and capillary trapping of CO_2 during drainage and imbibition processes in a micromodel. Zheng et al. (2017) used food coloring to tag brine in drainage experiments with CO_2 under liquid, gaseous and supercritical conditions.

Imaging can be carried out even without a fluorescent dye, using bright-field imaging, although with a lower signal-to-noise ratio. In this configuration, CO_2–water interfaces are visible due to their different refractive indices, and depending on the illumination source and imaging spectrum, the two fluid phases may have different signal intensity. In addition, information such as wetting properties or flow direction can be used to identify the fluid phases (Cao et al. 2016; Hu et al. 2017a, b; Jafari and Jung 2017; Kim et al. 2012c; Morais et al. 2016; Qin et al. 2017). Kim et al. (2012c) studied the changes in wettability of a glass micromodel due to exposure to scCO_2 and brine with different salinities. Cao et al. (2016) studied the effect of contact angle and salinity on displacement patterns in CO_2 drainage, and they compared the results with pore network numerical simulations. Morais et al. (2016) used high-speed imaging to resolve dynamic displacement patterns and evolution of CO_2 saturation for various subcritical and supercritical p–T combinations. Hu et al. (2017a) studied the effects of contact angle and flow rate on displacement patterns during CO_2 drainage, and they compared experimental results with numerical simulations solving the Navier–Stokes equations. Hu et al. (2017b) studied the effect of contact angle on spatial distribution and morphology of the trapped CO_2 phase during water imbibition for different flow rates. Jafari and Jung (2017) used micromodels to measure static as well as advancing and receding dynamic contact angles in a CO_2/water/glass system. Qin et al. (2017) studied flow of liquid CO_2 and water in a micro-T-junction, and Sell et al. (2013) measured diffusivity of CO_2 in water and 0–5 M NaCl solution using fluorescein at 26 °C and 5–50 bar.

4.3 Biomedical Sciences

Microfluidics can revolutionize current practices in cell biology (Paguirigan and Beebe 2008), in vitro cell culture studies (Barisam et al. 2017), pathophysiology (Wang et al. 2013b), biochemistry (Ohno et al. 2008), drug delivery (Nguyen et al. 2013), nanoparticle deposition (Moghadas et al. 2017b), oncology (Kashaninejad et al. 2016), assisted reproductive technology (Kashaninejad et al. 2018), hematology (Myers et al. 2012), immunology and antibody screening (Seah et al. 2017) and pharmacology (Delamarche et al. 2013). For instance, microfluidic devices can provide an in vivo-like microenvironment to culture cells in a dynamic and perfusion-based manner. Coupled with concentration gradient generators, microfluidic cell culture devices can facilitate high-throughput and high-content drug screening, thus opening a new era in personalized medicine. For cancer treatment, microfluidic platforms have shown a great promise in 3D tumor spheroid formation and culture (Moshksayan et al. 2018). At a single-cell level, microfluidic devices enable a versatile platform to address fundamental questions in biology. Droplet- and valve-based microfluidic devices

realize highly efficient and compartmentalized platforms to study individual cells, including the interaction of T-cell and B-cell receptors (Seah et al. 2018). The unique features of two commonly used formats of microfluidics, i.e., continuous-flow microfluidics or droplet-based microfluidics, in liquid handling can automate sophisticated bioassay protocols and facilitate mixing and separation of various biomedical samples for diagnostics and treatment (Gomez 2013; Nguyen et al. 2017; Sackmann et al. 2014). Proposed by Whiteside's group at Harvard University in 2009, microfluidic paper-based analytical devices (μPADs) are another format of microfluidics that can be used for diagnostic purposes (Martinez et al. 2009). They meet the ASSURED (affordable, sensitive, specific, user-friendly, rapid and robust, equipment-free and deliverable to end-users) criteria of World Health Organization and can be used as portable point-of-care diagnostic devices in resource-limited settings.

For tissue engineering and regenerative medicine, microfluidic cell culture bioreactors have also progressed rapidly. Accordingly, another format of microfluidic systems in biomedical science named as organ-on-a-chip has emerged (Moraes et al. 2012). Organ-on-a-chip devices with a semipermeable porous membrane, which was discussed previously, have provided a platform that can bridge the gap between animal studies and in vitro cell culture models (Bhatia and Ingber 2014; Huh et al. 2013). These membranes have been used in various organ-on-a-chip platforms for disease modeling and drug screening (Huh et al. 2011). These platforms include lung-on-a-chip (Huh et al. 2010), gut-on-a-chip (Kim et al. 2012b), liver-on-a-chip (Prodanov et al. 2016), kidney-on-a-chip (Nieskens and Wilmer 2016), blood–brain barrier-on-a-chip (van der Helm et al. 2016) and placenta-on-a-chip (Lee et al. 2016).

Other than organ-on-a-chip, membrane-based microfluidic devices can be used in cell/particle sorting by implementing strategies of size-based filtration. Efficient particle/cell sorting is an essential step in most clinical, biological and industrial processes. To this end, both active and passive techniques can be used. Although the separation efficiency and selectivity can be better controlled using active techniques, these techniques require external forces that compromise the portability and simplicity of the device. Among various passive techniques, size-based filtration using isoporous membranes embedded in a microfluidic device have attracted significant attention. These devices have several applications including emulsion separation (Vladisavljević et al. 2012), drug delivery (Yang et al. 2010), water purification (Warkiani et al. 2011) and pathogen detection for food safety (Yoon and Kim 2012). Both in situ and off-chip techniques can be used to fabricate and integrate these membranes into microfluidic devices. Although in situ techniques such as femtosecond laser multi-foci parallel microfabrication (Xu et al. 2016) are elegant and can significantly reduce production time, their poor controllability over membrane pore size and difficulty in precisely positioning the membrane limit their application.

Size-based filtration using membrane-based microfluidics can be used for cancer diagnostics (Dong et al. 2013). Of particular interest is the application of minimally invasive techniques to detect cancer biomarkers in the blood known as liquid biopsy (Zhang et al. 2017). Among cancer biomarkers, circulating tumor cells (CTCs) proved to be a better candidate for diagnostic and prognostic of cancer (Warkiani et al. 2014a). Accordingly, using microfluidic devices can offer significant advantages for label-free detection of viable CTCs from peripheral blood (Warkiani et al. 2014b). To this end, size-based filtration using a porous membrane integrated inside a microfluidic device is a practical approach. The membrane used for such a device should be highly porous with precise control over the pore size. Silicon-based membranes that are fabricated using photolithography were among the first membranes which met the necessary conditions for efficient CTCs detection (Lim et al. 2012). Fan et al. (2015) used water-dissolvable polyvinyl alcohol (PVA) as supporting (and sacrificial) layer for PDMS soft lithography to fabricate a thin and highly porous PDMS membrane. As shown

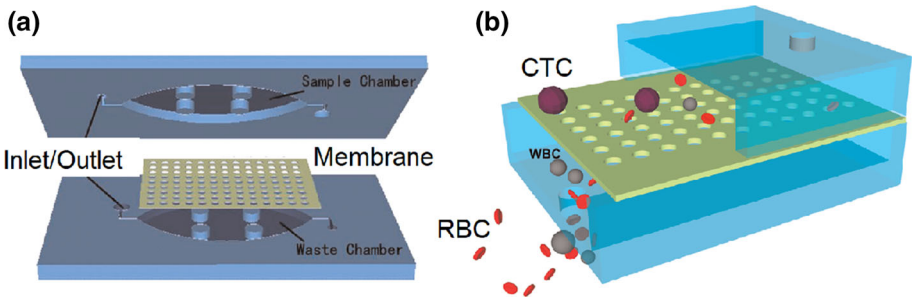

Fig. 9 Schematic of membrane-based microfluidic devices used to isolate CTCs. **a** Porous membrane sandwiched between sample channel and waster channel. **b** Illustration of sized-based filtration method to isolate CTCs from RBCs and WBCs. Reproduced with permission from Fan et al. (2015)

in Fig. 9, the membrane was then used inside a microfluidic device to separate CTCs from white blood cells (WBCs) and red blood cells (RBCs). They reported a capture efficiency of more than 90% using this technique.

To improve the release efficiency of the captured CTCs for further molecular analysis, Kim et al. (2016) used a releasing agent, poly(ethylene glycol) (PEG), on the SU8 microfilter. They showed over 20% improvement in releasing the captured CTCs from the whole blood sample. Kang et al. (2017) fabricated a photosensitive polymer-based microfilter and attached the filter to a syringe to rapidly isolate viable CTCs. They reported a CTC capture efficiency of over 75% from the whole blood samples with over 80% viability. Nevertheless, the efficiency of microfiltration-based CTC isolation techniques is highly dependent on the pore size, and it is limited to CTCs larger than the pore size (Zhang et al. 2016).

5 Future Directions

The development of microfluidics techniques is continually enhancing biological, medical, environmental and engineering technologies in many aspects. Samples can be prepared and analyzed at low volumes to replace heavy, large and expensive equipment and manual processing. Based on the extensive knowledge in microfluidic techniques, chips with specific applications can be designed, fabricated and commercialized. During the past two decades, the commercialization of microfluidics in biomedical science has been rapidly growing and on-a-chip devices have been introduced to the market for many techniques including genome sequencing and in vitro diagnostics (Volpatti and Yetisen 2014). In the oil and gas industry, lab-on-a-chip devices are also advancing, such as the commercialization of a microfluidic device for the measurement of asphaltene content in crude oil (Sieben et al. 2013). Other companies are producing and commercializing miniaturized analytical devices for various applications (Haber 2006). These applications will reduce the cost and time for the fabrication of microfluidic devices and thus increase the adoption of this technology for industrial applications. In particular, new opportunities in automation and rapid analysis or screening procedures for a variety of different engineering applications are a promising way forward.

We need to combine and integrate recent advances and innovations from various disciplines in biomedical science, chemistry, hydrology and petroleum engineering, which can be merged for the production of fully integrated and/or functionalized devices. For instance, developments in surface functionalization, chemical processes and catalyst performance

from chemistry and biomedical sciences could be important for developing microfluidic chips with the surface wetting properties required to study a given EOR process. In addition, the development of geomaterial chips could be utilized for etching biomedical scaffoldings for depositing cells. Last, membrane technologies for advanced sorting and filtration in the biomedical sciences are also largely important for water treatment processes and/or potential separation of crude oil components for processing and/or analytical analyses. Microfluidics can be implemented in order to address engineering problems that lack conventional setups for observation, diagnostic, or analysis. Cooperation of academics and industrial companies will play an important role in the identification of potential objectives in which microfluidics can help to address them. Other than commercializing microfluidic devices, advanced visualization and analysis setups offered by microfluidics can provide new insights into unknown mechanisms that occur in porous media. They can facilitate the analysis of simulation capabilities where multiple phases and components are being transported with unique equations of state and/or where standard assumptions of local equilibrium can no longer be applied. The future of microfluidic studies is indeed an exciting area of research and will remain as an essential tool for porous media studies and engineering applications.

References

Adrian, R.J., Westerweel, J.: Particle Image Velocimetry. Cambridge University Press, Cambridge (2011)

Ahmed, F.E., Lalia, B.S., Hashaikeh, R.: A review on electrospinning for membrane fabrication: challenges and applications. Desalination **356**, 15–30 (2015)

Alagorni, A.H., Yaacob, Z., Nour, A.H.: An overview of oil production stages: enhanced oil recovery techniques and nitrogen injection. Int. J. Environ. Sci. Dev. **6**(9), 693–701 (2015)

Albani, J.R.: Structure and Dynamics of Macromolecules: Absorption and Fluorescence Studies. Elsevier, Amsterdam (2011)

Albaugh, K.B.: Electrode phenomena during anodic bonding of silicon to sodium borosilicate glass. J. Electrochem. Soc. **138**(10), 3089–3094 (1991)

Alzahid, Y., et al.: Alkaline surfactant polymer flooding: what happens at the pore scale? In: SPE Europec Featured at 79th EAGE Conference and Exhibition. Society of Petroleum Engineers (2017)

Alzahid, Y.A., et al.: Functionalisation of polydimethylsiloxane (PDMS)—microfluidic devices coated with rock minerals. Sci. Rep. **8**(1), 15518 (2018)

Alzahid, Y.A., Mostaghimi, P., Walsh, S.D.C., Armstrong, R.T.: Flow regimes during surfactant flooding: the influence of phase behaviour. Fuel **236**, 851–860 (2019)

Amirian, T., Haghighi, M., Mostaghimi, P.: Pore scale visualization of low salinity water flooding as an enhanced oil recovery method. Energy Fuels **31**, 13133–13143 (2017)

Anbari, A., et al.: Microfluidic model porous media: fabrication and applications. Small **14**(18), 1703575 (2018)

Armstrong, R.T., Berg, S.: Interfacial velocities and capillary pressure gradients during Haines jumps. Phys. Rev. E **88**(4), 043010 (2013)

Atencia, J., Beebe, D.: Controlled microfluidic interfaces. Nature **437**, 648–655 (2005)

Bachu, S.: Sequestration of CO_2 in geological media: criteria and approach for site selection in response to climate change. Energy Convers. Manag. **41**(9), 953–970 (2000)

Barisam, M., Saidi, M., Kashaninejad, N., Vadivelu, R., Nguyen, N.-T.: Numerical simulation of the behavior of toroidal and spheroidal multicellular aggregates in microfluidic devices with microwell and U-shaped barrier. Micromachines **8**(12), 358 (2017)

Bartels, W.-B., et al.: Oil configuration under high-salinity and low-salinity conditions at pore scale: a parametric investigation by use of a single-channel micromodel. SPE J. **22**(05), 1362–1373 (2017)

Bartels, W.B., et al.: Low salinity flooding (LSF) in sandstones at pore scale: micro-model development and investigation. In: SPE Annual Technical Conference and Exhibition. Society of Petroleum Engineers, p. 17, Dubai (2016)

Basabe-Desmonts, L., et al.: A simple approach to sensor discovery and fabrication on self-assembled monolayers on glass. J. Am. Chem. Soc. **126**(23), 7293–7299 (2004)

Berkowski, K.L., Plunkett, K.N., Yu, Q., Moore, J.S.: Introduction to photolithography: preparation of microscale polymer silhouettes. J. Chem. Educ. **82**(9), 1365 (2005)
Bhatia, S.N., Ingber, D.E.: Microfluidic organs-on-chips. Nat. Biotechnol. **32**(8), 760–772 (2014)
Biswas, R., Lewis, J.E., Maroncelli, M.: Electronic spectral shifts, reorganization energies, and local density augmentation of Coumarin 153 in supercritical solvents. Chem. Phys. Lett. **310**, 485–494 (1999)
Booth, R., Kim, H.: Characterization of a microfluidic in vitro model of the blood–brain barrier (μBBB). Lab Chip **12**(10), 1784–1792 (2012)
Bowden, S.A., Tanino, Y., Akamairo, B., Christensen, M.: Recreating mineralogical petrographic heterogeneity within microfluidic chips: assembly, examples, and applications. Lab Chip **16**(24), 4677–4681 (2016)
Brian, J.K., Ellis, M.: Review of polymer MEMS micromachining. J. Micromech. Microeng. **26**(1), 013001 (2016)
Britt, L.K., Schoeffler, J.: The Geomechanics of a Shale Play: What Makes a Shale Prospective. Society of Petroleum Engineers, New York (2009)
Buchgraber, M., Kovscek, A.R., Castanier, L.M.: A study of microscale gas trapping using etched silicon micromodels. Transp. Porous Media **95**(3), 647–668 (2012)
Cao, S.C., Dai, S., Jung, J.: Supercritical CO_2 and brine displacement in geological carbon sequestration: micromodel and pore network simulation studies. Int. J. Greenhouse Gas Control **44**(6), 104–114 (2016)
Chang, C., et al.: Pore-scale supercritical CO_2 dissolution and mass transfer under imbibition conditions. Adv. Water Resour. **92**(March), 142–158 (2016)
Chang, C., Zhou, Q., Oostrom, M., Kneafsey, T.J., Mehta, H.: Pore-scale supercritical CO_2 dissolution and mass transfer under drainage conditions. Adv. Water Resour. **100**, 14–25 (2017)
Chapman, E.M., Yang, J., Crawshaw, J.P., Boek, E.S.: Pore scale models for imbibition of CO_2 analogue fluids in etched micro-model junctions using micro-fluidic experiments and direct flow calculations. Energy Proc. **37**, 3680–3686 (2013)
Chen, Y.: Nanofabrication by electron beam lithography and its applications: a review. Microelectron. Eng. **135**, 57–72 (2015)
Chen, Y., Li, Y., Valocchi, A.J., Christensen, K.T.: Lattice Boltzmann simulations of liquid CO_2 displacing water in a 2D heterogeneous micromodel at reservoir pressure conditions. J. Contam. Hydrol. **53**, 6178–6196 (2017)
Chrimes, A.F., Khoshmanesh, K., Stoddart, P.R., Mitchell, A., Kalantar-zadeh, K.: Microfluidics and Raman microscopy: current applications and future challenges. Chem. Soc. Rev. **42**(13), 5880–5906 (2013)
Christensen, K.: The influence of peak-locking errors on turbulence statistics computed from PIV ensembles. Exp. Fluids **36**(3), 484–497 (2004)
Datta, S., Chiang, H., Ramakrishnan, T.S., Weitz, D.: Spatial fluctuations of fluid velocities in flow through a three-dimensional porous medium. Phys. Rev. Lett. **111**, 064501 (2013)
Datta, S.S., Dupin, J.-B., Weitz, D.A.: Fluid breakup during simultaneous two-phase flow through a three-dimensional porous medium. Phys. Fluids **26**(6), 062004 (2014)
Davies, M.J., Marques, M.P.C., Radhakrishnan, A.N.P.: Chapter 2 Microfluidics Theory in Practice, Microfluidics in Detection Science: Lab-on-a-chip Technologies, pp. 29–60. The Royal Society of Chemistry, New York (2015)
de Haas, T.W., Fadaei, H., Guerrero, U., Sinton, D.: Steam-on-a-chip for oil recovery: the role of alkaline additives in steam assisted gravity drainage. Lab Chip **13**(19), 3832–3839 (2013)
Deckert, V., et al.: Spatial resolution in Raman spectroscopy. Faraday Discuss. **177**, 9–20 (2015)
Delamarche, E., Tonna, N., Lovchik, R.D., Bianco, F., Matteoli, M.: Pharmacology on microfluidics: multimodal analysis for studying cell–cell interaction. Curr. Opin. Pharmacol. **13**(5), 821–828 (2013)
Dong, M., Liu, Q., Li, A.: Displacement mechanisms of enhanced heavy oil recovery by alkaline flooding in a micromodel. Particuology **10**(3), 298–305 (2012)
Dong, Y., et al.: Microfluidics and circulating tumor cells. J. Mol. Diagn. **15**(2), 149–157 (2013)
Doughty, M.J.: pH dependent spectral properties of sodium fluorescein ophthalmic solutions revisited. Ophthalmic Physiol. Opt. **30**(2), 167–174 (2010)
Fakhari, A., Li, Y., Bolster, D., Christensen, K.T.: A phase-field lattice Boltzmann model for simulating multiphase flows in porous media: application and comparison to experiments of CO_2 sequestration at pore scale. Adv. Water Resour. **114**, 119–134 (2018)
Fan, X., et al.: A microfluidic chip integrated with a high-density PDMS-based microfiltration membrane for rapid isolation and detection of circulating tumor cells. Biosens. Bioelectron. **71**, 380–386 (2015)
Franssila, S.: Introduction to Microfabrication. Wiley (2010)
Friend, J., Yeo, L.: Fabrication of microfluidic devices using polydimethylsiloxane. Biomicrofluidics **4**(2), 026502 (2010)
Gerami, A., et al.: Microscale insights into gas recovery from bright and dull bands in coal. J. Petrol. Sci. Eng. **172**, 373–382 (2018)

Gerami, A., et al.: Coal-on-a-chip: visualizing flow in coal fractures. Energy Fuels **31**(10), 10393–10403 (2017)
Gerami, A., Mostaghimi, P., Armstrong, R.T., Zamani, A., Warkiani, M.E.: A microfluidic framework for studying relative permeability in coal. Int. J. Coal Geol. **159**, 183–193 (2016)
Giboz, J., Copponnex, T., Mélé, P.: Microinjection molding of thermoplastic polymers: a review. J. Micromech. Microeng. **17**(6), R96 (2007)
Godinez-Brizuela, O.E., Karadimitriou, N.K., Joekar-Niasar, V., Shore, C.A., Oostrom, M.: Role of corner interfacial area in uniqueness of capillary pressure-saturation- interfacial area relation under transient conditions. Adv. Water Resour. **107**, 10–21 (2017)
Gomez, F.A.: The future of microfluidic point-of-care diagnostic devices. Bioanalysis **5**(1), 1–3 (2013)
Gravesen, P., Branebjerg, J., Jensen, O.S.: Microfluidics—a review. J. Micromech. Microeng. **3**(4), 168 (1993)
Guckenberger, D.J., de Groot, T.E., Wan, A.M.D., Beebe, D.J., Young, E.W.K.: Micromilling: a method for ultra-rapid prototyping of plastic microfluidic devices. Lab Chip **15**(11), 2364–2378 (2015)
Gunda, N.S., Bera, B., Karadimitriou, N.K., Mitra, S.K., Hassanizadeh, S.M.: Reservoir-on-a-chip (ROC): a new paradigm in reservoir engineering. Lab Chip **11**(22), 3785–3792 (2011)
Guo, H., et al.: Quantitative Raman spectroscopic investigation of geo-fluids high-pressure phase equilibria: part I. Accurate calibration and determination of CO_2 solubility in water from 273.15 to 573.15 K and from 10 to 120 MPa. Fluid Phase Equilib. **382**, 70–79 (2014)
Guo, H., Huang, Y., Chen, Y., Zhou, Q.: Quantitative Raman spectroscopic measurements of CO_2 solubility in NaCl solution from (273.15 to 473.15) K at p = (10.0, 20.0, 30.0, and 40.0) MPa. J. Chem. Eng. Data **61**(1), 466–474 (2015)
Haber, C.: Microfluidics in commercial applications; an industry perspective. Lab Chip **6**(9), 1118–1121 (2006)
Hae Choi, Y., et al.: Effect of functional groups on the solubilities of coumarin derivatives in supercritical carbon dioxide. Chromatographia **47**(1–2), 93–97 (1998)
Haeberle, S., Zengerle, R.: Microfluidic platforms for lab-on-a-chip applications. Lab Chip **7**(9), 1094–1110 (2007)
Haszeldine, R.S.: Carbon capture and storage: how green can black be? Science (New York) **325**(5948), 1647–1652 (2009)
He, K., Xu, L., Gao, Y., Yin, X., Neeves, K.B.: Evaluation of surfactant performance in fracturing fluids for enhanced well productivity in unconventional reservoirs using rock-on-a-Chip approach. J. Petrol. Sci. Eng. **135**, 531–541 (2015)
He, K., Xu, L., Kenzhekhanov, S., Yin, X., Neeves, K.B.: A Rock-on-a-Chip Approach to Study Fluid Invasion and Flowback in Liquids-Rich Shale Formations. Society of Petroleum Engineers, London (2017)
Hematpour, H., Mardi, M., Edalatkhah, S., Arabjamaloei, R.: Experimental study of polymer flooding in low-viscosity oil using one-quarter five-spot glass micromodel. Pet. Sci. Technol. **29**(11), 1163–1175 (2011)
Hilic, S., Boyer, S.V.A.E., AlAH, Pádua, Grolier, J.P.E.: Simultaneous measurement of the solubility of nitrogen and carbon dioxide in polystyrene and of the associated polymer swelling. J. Polym. Sci. Part B: Polym. Phys. **39**(17), 2063–2070 (2001)
Homsy, G.M.: Viscous fingering in porous media. Annu. Rev. Fluid Mech. **19**(1), 271–311 (1987)
Hu, R., Wan, J., Kim, Y., Tokunaga, T.K.: Wettability effects on supercritical CO_2–brine immiscible displacement during drainage: pore-scale observation and 3D simulation. Int. J. Greenhouse Gas Control **60**, 129–139 (2017a)
Hu, R., Wan, J., Kim, Y., Tokunaga, T.K.: Wettability Impact on Supercritical CO_2 Capillary Trapping: Pore-Scale Visualization and Quantification. Water Resources Research, London (2017b)
Huh, D., Hamilton, G.A., Ingber, D.E.: From 3D cell culture to organs-on-chips. Trends Cell Biol. **21**(12), 745–754 (2011)
Huh, D., et al.: Microfabrication of human organs-on-chips. Nat. Protoc. **8**(11), 2135–2157 (2013)
Huh, D., et al.: Reconstituting organ-level lung functions on a chip. Science **328**(5986), 1662–1668 (2010)
Huppert, H.E., Neufeld, J.A.: The fluid mechanics of carbon dioxide sequestration. Annu. Rev. Fluid Mech. **46**(1), 255–272 (2014)
Iliescu, C., Taylor, H., Avram, M., Miao, J., Franssila, S.: A practical guide for the fabrication of microfluidic devices using glass and silicon. Biomicrofluidics **6**(1), 016505–016505-16 (2012)
Jacob, R., Saylor, B.Z.: CO_2 solubility in multi-component brines containing NaCl, KCl, CaCl 2 and MgCl 2 at 297 K and 1–14MPa. Chem. Geol. **424**, 86–95 (2016)
Jafari, M., Jung, J.: Direct measurement of static and dynamic contact angles using a random micromodel considering geological CO_2 sequestration. Sustainability **9**(12), 2352 (2017)
Jahanshahi, A., Salvo, P., Vanfleteren, J.: PDMS selective bonding for the fabrication of biocompatible all polymer NC microvalves. J. Microelectromech. Syst. **22**(6), 1354–1360 (2013)

Jiang, C., Tsukruk, V.V.: Freestanding nanostructures via layer-by-layer assembly. Adv. Mater. **18**(7), 829–840 (2006)

Kalkandjiev, K., Gutzweiler, L., Welsche, M., Zengerle, R., Koltay, P.: A novel approach for the fabrication of all-polymer microfluidic devices. In: 2010 IEEE 23rd International Conference on Micro Electro Mechanical Systems (MEMS), pp. 1079–1082. IEEE (2010)

Kang, Y.-T., Doh, I., Byun, J., Chang, H.J., Cho, Y.-H.: Label-free rapid viable enrichment of circulating tumor cell by photosensitive polymer-based microfilter device. Theranostics **7**(13), 3179 (2017)

Karadimitriou, N.K., Hassanizadeh, S.M.: A review of micromodels and their use in two-phase flow studies. Vadose Zone J. **11**(3), 85 (2012)

Karadimitriou, N.K., Hassanizadeh, S.M., Joekar-Niasar, V., Kleingeld, P.J.: Micromodel study of two-phase flow under transient conditions: quantifying effects of specific interfacial area. Water Resour. Res. **50**(10), 8125–8140 (2014)

Karadimitriou, N.K., Joekar-Niasar, V., Hassanizadeh, S.M., Kleingeld, P.J., Pyrak-Nolte, L.J.: A novel deep reactive ion etched (DRIE) glass micro-model for two-phase flow experiments. Lab Chip **12**(18), 3413–3418 (2012)

Karadimitriou, N.K., et al.: On the fabrication of PDMS micromodels by rapid prototyping, and their use in two-phase flow studies. Water Resour. Res. **49**(4), 2056–2067 (2013)

Kashaninejad, N., et al.: Organ-tumor-on-a-chip for chemosensitivity assay: a critical review. Micromachines **7**(8), 130 (2016)

Kashaninejad, N., Shiddiky, M.J.A., Nguyen, N.-T.: Advances in microfluidics-based assisted reproductive technology: from sperm sorter to reproductive system-on-a-chip. Advanced Biosystems **2**(1), 1700197 (2018)

Kawata, S., Ichimura, T., Taguchi, A., Kumamoto, Y.: Nano-Raman scattering microscopy: resolution and enhancement. Chem. Rev. **117**(7), 4983–5001 (2017)

Kazemifar, F., Blois, G., Kyritsis, D.C., Christensen, K.T.: A methodology for velocity field measurement in multiphase high-pressure flow of CO_2 and water in micromodels. Water Resour. Res. **51**(4), 3017–3029 (2015)

Kazemifar, F., Blois, G., Kyritsis, D.C., Christensen, K.T.: Quantifying the flow dynamics of supercritical CO_2–water displacement in a 2D porous micromodel using fluorescent microscopy and microscopic PIV. Adv. Water Resour. **95**, 352–368 (2016)

Kazemifar, F., Kyritsis, D.C.: Experimental investigation of near-critical CO_2 tube-flow and Joule-Thompson throttling for carbon capture and sequestration. Exp. Therm. Fluid Sci. **53**, 161–170 (2014)

Kim, D., et al.: Reaction-based two-photon probes for in vitro analysis and cellular imaging of monoamine oxidase activity. Chem. Commun. **48**(54), 6833–6835 (2012a)

Kim, H.J., Huh, D., Hamilton, G., Ingber, D.E.: Human gut-on-a-chip inhabited by microbial flora that experiences intestinal peristalsis-like motions and flow. Lab Chip **12**(12), 2165–2174 (2012b)

Kim, Y., Wan, J., Kneafsey, T.J., Tokunaga, T.K.: Dewetting of silica surfaces upon reactions with supercritical CO_2 and brine: pore-scale studies in micromodels. Environ. Sci. Technol. **46**(7), 4228–4235 (2012c)

Kim, H.N., Lee, M.H., Kim, H.J., Kim, J.S., Yoon, J.: A new trend in rhodamine-based chemosensors: application of spirolactam ring-opening to sensing ions. Chem. Soc. Rev. **37**(8), 1465–1472 (2008a)

Kim, P., Kwon, K.W., Park, M.C., Lee, S.H., Kim, S.M., Suh, K.Y.: Soft lithography for microfluidics: a review. Biochip J. **2**(1), 1–11 (2008b)

Kim, H.N., et al.: Rhodamine hydrazone derivatives as Hg2 + selective fluorescent and colorimetric chemosensors and their applications to bioimaging and microfluidic system. Analyst **136**(7), 1339–1343 (2011)

Kim, Y.J., Kang, Y.-T., Cho, Y.-H.: Poly(ethylene glycol)-modified tapered-slit membrane filter for efficient release of captured viable circulating tumor cells. Anal. Chem. **88**(16), 7938–7945 (2016)

Kim, M., Abedini, A., Lele, P., Guerrero, A., Sinton, D.: Microfluidic pore-scale comparison of alcohol- and alkaline-based SAGD processes. J. Petrol. Sci. Eng. **154**, 139–149 (2017)

King, M.B.B., Mubarak, A., Kim, J.D.D., Bott, T.R.R.: The mutual solubilities of water with supercritical and liquid carbon dioxides. J. Supercrit. Fluids **5**(4), 296–302 (1992)

Kjeang, E., Djilali, N., Sinton, D.: Microfluidic fuel cells: a review. J. Power Sour. **186**(2), 353–369 (2009)

Laerme, F., Schilp, A., Funk, K., Offenberg, M.: Bosch deep silicon etching: improving uniformity and etch rate for advanced MEMS applications. In: 12th IEEE International Conference on Micro Electro Mechanical Systems, 1999. MEMS'99, pp. 211–216. IEEE (1999)

Lake, L.W.: Enhanced Oil Recovery. Prentice Hall, Englewood Cliffs (2014)

Le-The, H., et al.: Large-scale fabrication of free-standing and sub-[small mu]m PDMS through-hole membranes. Nanoscale **10**(16), 7711–7718 (2018)

Lee, J.S., et al.: Placenta-on-a-chip: a novel platform to study the biology of the human placenta. J. Matern. Fetal Neonatal Med. **29**(7), 1046–1054 (2016)

Lee Seung, G., Lee, H., Gupta, A., Chang, S., Doyle Patrick, S.: Site-selective in situ grown calcium carbonate micromodels with tunable geometry, porosity, and wettability. Adv. Func. Mater. **26**(27), 4896–4905 (2016)
Lei, K.F.: Chapter 1 Materials and Fabrication Techniques for Nano- and Microfluidic Devices, Microfluidics in Detection Science: Lab-on-a-chip Technologies, pp. 1–28. The Royal Society of Chemistry, New York (2015)
Leis, A.P., Schlicher, S., Franke, H., Strathmann, M.: Optically transparent porous medium for nondestructive studies of microbial biofilm architecture and transport dynamics. Appl. Environ. Microbiol. **71**(8), 4801–4808 (2005)
Lenormand, R., Touboul, E., Zarcone, C.: Numerical models and experiments on immiscible displacements in porous media. J. Fluid Mech. **189**, 165–187 (1988)
Li, X., Wu, N., Rojanasakul, Y., Liu, Y.: Selective stamp bonding of PDMS microfluidic devices to polymer substrates for biological applications. Sens. Actuators A **193**, 186–192 (2013)
Li, Y., Kazemifar, F., Blois, G., Christensen, K.T.: Micro-PIV measurements of multiphase flow of water and liquid CO_2 in 2-D heterogeneous porous micromodels. Water Resour. Res. **53**(7), 6178–6196 (2017)
Lim, L.S., et al.: Microsieve lab-chip device for rapid enumeration and fluorescence in situ hybridization of circulating tumor cells. Lab Chip **12**(21), 4388–4396 (2012)
Liu, N., Aymonier, C., Lecoutre, C., Garrabos, Y., Marre, S.: Microfluidic approach for studying CO_2 solubility in water and brine using confocal Raman spectroscopy. Chem. Phys. Lett. **551**, 139–143 (2012)
Liu, M., Shabaninejad, M., Mostaghimi, P.: Impact of mineralogical heterogeneity on reactive transport modelling. Comput. Geosci. **104**(Supplement C), 12–19 (2017)
Lu, C., Lee, L.J., Juang, Y.J.: Packaging of microfluidic chips via interstitial bonding technique. Electrophoresis **29**(7), 1407–1414 (2008)
Lu, W., Guo, H., Chou, I.M., Burruss, R.C., Li, L.: Determination of diffusion coefficients of carbon dioxide in water between 268 and 473 K in a high-pressure capillary optical cell with in situ Raman spectroscopic measurements. Geochim. Cosmochim. Acta **115**, 183–204 (2013)
Madou, M.J.: Fundamentals of Microfabrication: The Science of Miniaturization. CRC Press, Boca Raton (2002)
Mahoney, S.A., Rufford, T.E., Dmyterko, A.S.K., Rudolph, V., Steel, K.M.: The effect of rank and lithotype on coal wettability and its application to coal relative permeability models. In: SPE Asia Pacific Unconventional Resources Conference and Exhibition, Brisbane
Mahoney, S.A., et al.: The effect of rank, lithotype and roughness on contact angle measurements in coal cleats. Int. J. Coal Geol. **179**, 302–315 (2017)
Martin, M.M., Lindqvist, L.: The pH dependence of fluorescein fluorescence. J. Lumin. **10**(6), 381–390 (1975)
Martínez-Máñez, R., Sancenón, F.: Fluorogenic and chromogenic chemosensors and reagents for anions. Chem. Rev. **103**(11), 4419–4476 (2003)
Martinez, A.W., Phillips, S.T., Whitesides, G.M., Carrilho, E.: Diagnostics for the developing world: microfluidic paper-based analytical devices. Anal. Chem. **82**(1), 3–10 (2009)
McDonald, J.C., et al.: Fabrication of microfluidic systems in poly(dimethylsiloxane). Electrophoresis **21**(1), 27–40 (2000)
Meinhart, C.D., Wereley, S.T., Santiago, J.G.: PIV measurements of a microchannel flow. Exp. Fluids **27**(5), 414–419 (1999)
Mela, P., et al.: Monolayer-functionalized microfluidics devices for optical sensing of acidity. Lab Chip **5**(2), 163–170 (2005)
Moebius, F., Or, D.: Interfacial jumps and pressure bursts during fluid displacement in interacting irregular capillaries. J. Colloid Interface Sci. **377**(1), 406–415 (2012)
Moebius, F., Or, D.: Pore scale dynamics underlying the motion of drainage fronts in porous media. Water Resour. Res. **50**(11), 8441–8457 (2014)
Moghadas, H., Saidi, M.S., Kashaninejad, N., Kiyoumarsioskouei, A., Nguyen, N.-T.: Fabrication and characterization of low-cost, bead-free, durable and hydrophobic electrospun membrane for 3D cell culture. Biomed. Microdevice **19**(4), 74 (2017a)
Moghadas, H., Saidi, M.S., Kashaninejad, N., Nguyen, N.-T.: Challenge in particle delivery to cells in a microfluidic device. Drug Deliv. Transl. Res. (2017b). https://doi.org/10.1007/s13346-017-0467-3
Moghadas, H., Saidi, M.S., Kashaninejad, N., Nguyen, N.-T.: A high-performance polydimethylsiloxane electrospun membrane for cell culture in lab on a chip. Biomicrofluidics **12**(2), 024117 (2018)
Mohammadzadeh, O., Chatzis, I.: Analysis of the heat losses associated with the SAGD visualization experiments. J. Petrol. Explor. Prod. Technol. **6**(3), 387–400 (2016)
Mohammadzadeh, O., Rezaei, N., Chatzis, I.: Pore-level investigation of heavy oil and Bitumen recovery using solvent—aided steam assisted gravity drainage (SA-SAGD) process. Energy Fuels **24**(12), 6327–6345 (2010)

Moraes, C., Mehta, G., Lesher-Perez, S.C., Takayama, S.: Organs-on-a-chip: a focus on compartmentalized microdevices. Ann. Biomed. Eng. **40**(6), 1211–1227 (2012)
Morais, S., Diouf, A., Lecoutre, C., Bernard, D., Garrabos, Y., Marre, S.: Geological labs on chip-new tools for investigating key aspects of CO_2 geological storage. In: The Third Sustainable Earth Sciences Conference and Exhibition (2015)
Morais, S., et al.: Monitoring CO_2 invasion processes at the pore scale using geological labs on chip. Lab Chip **16**(18), 3493–3502 (2016)
Morin, B., Liu, Y., Alvarado, V., Oakey, J.: A microfluidic flow focusing platform to screen the evolution of crude oil-brine interfacial elasticity. Lab Chip **16**(16), 3074–3081 (2016)
Moshksayan, K., et al.: Spheroids-on-a-chip: recent advances and design considerations in microfluidic platforms for spheroid formation and culture. Sens. Actuators B Chem. **263**, 151–176 (2018)
Myers, D.R., et al.: Endothelialized microfluidics for studying microvascular interactions in hematologic diseases. J. Vis. Exp. (JoVE) **64**, 3958 (2012)
Nan, Z., et al.: Manufacturing microstructured tool inserts for the production of polymeric microfluidic devices. J. Micromech. Microeng. **25**(9), 095005 (2015)
Nguyen, C., Kothamasu, R., He, K., Xu, L.: Low-Salinity Brine Enhances Oil Production in Liquids-Rich Shale Formations. Society of Petroleum Engineers, London (2015)
Nguyen, N.-T., Hejazian, M., Ooi, C.H., Kashaninejad, N.: Recent advances and future perspectives on microfluidic liquid handling. Micromachines **8**, 186 (2017)
Nguyen, N.-T., Shaegh, S.A.M., Kashaninejad, N., Phan, D.-T.: Design, fabrication and characterization of drug delivery systems based on lab-on-a-chip technology. Adv. Drug Deliv. Rev. **65**(11–12), 1403–1419 (2013)
Nieskens, T.T., Wilmer, M.J.: Kidney-on-a-chip technology for renal proximal tubule tissue reconstruction. Eur. J. Pharmacol. **790**, 46–56 (2016)
Nolan, E.M., Lippard, S.J.: Tools and tactics for the optical detection of mercuric ion. Chem. Rev. **108**(9), 3443–3480 (2008)
Nordbotten, J.M., Celia, M.A., Bachu, S.: Injection and storage of CO_2 in deep saline aquifers: analytical solution for CO_2 plume evolution during injection. Transp. Porous Media **58**(3), 339–360 (2005)
Oh, Y.S., Jo, H.Y., Ryu, J.-H., Kim, G.-Y.: A microfluidic approach to water–rock interactions using thin rock sections: Pb and U sorption onto thin shale and granite sections. J. Hazard. Mater. B **324**, 373–381 (2017)
Ohno, K.I., Tachikawa, K., Manz, A.: Microfluidics: applications for analytical purposes in chemistry and biochemistry. Electrophoresis **29**(22), 4443–4453 (2008)
Olsen, M.G., Adrian, R.J.: Out-of-focus effects on particle image visibility and correlation in microscopic particle image velocimetry. Exp. Fluids **29**(7), S166–S174 (2000)
Pacala, S., Socolow, R.: Stabilization wedges: solving the climate problem for the next 50 years with current technologies. Science **305**(5686), 968–972 (2004)
Paguirigan, A.L., Beebe, D.J.: Microfluidics meet cell biology: bridging the gap by validation and application of microscale techniques for cell biological assays. BioEssays **30**(9), 811–821 (2008)
Pei, H., Zhang, G., Ge, J., Jin, L., Ma, C.: Potential of alkaline flooding to enhance heavy oil recovery through water-in-oil emulsification. Fuel **104**, 284–293 (2013)
Pensabene, V., et al.: Ultrathin polymer membranes with patterned, micrometric pores for organs-on-chips. ACS Appl. Mater. Interfaces **8**(34), 22629–22636 (2016)
Porter, M.L., et al.: Fundamental Investigation of Gas Injection in Microfluidic Shale Fracture Networks at Geologic Conditions. American Rock Mechanics Association, New York (2015a)
Porter, M.L., et al.: Geo-material microfluidics at reservoir conditions for subsurface energy resource applications. Lab Chip **15**, 4044–4053 (2015b)
Prodanov, L., et al.: Long-term maintenance of a microfluidic 3D human liver sinusoid. Biotechnol. Bioeng. **113**(1), 241–246 (2016)
Qin, N., Wen, J.Z., Ren, C.L.: Highly pressurized partially miscible liquid–liquid flow in a micro-*T*-junction. I. Exp. Obser. Phys. Rev. E **95**(4), 043110 (2017)
Raffel, M., Willert, C.E., Wereley, S.T., Kompenhans, J.: Particle Image Velocimetry: A Practical Guide. Springer, Berlin (2013)
Rangel-German, E., Kovscek, A.: A micromodel investigation of two-phase matrix-fracture transfer mechanisms. Water Resour. Res. **42**(3), 1 (2006)
Rindfleisch, F., DiNoia, T.P., McHugh, M.A.: Solubility of polymers and copolymers in supercritical CO_2. J. Phys. Chem. **100**(38), 15581–15587 (1996)
Rodríguez, S.J., Bishop, P.L.: Three-dimensional quantification of soil biofilms using image analysis. Environ. Eng. Sci. **24**(1), 96–103 (2007)
Sackmann, E.K., Fulton, A.L., Beebe, D.J.: The present and future role of microfluidics in biomedical research. Nature **507**(7491), 181–189 (2014)

Santiago, J.G., Wereley, S.T., Meinhart, C.D., Beebe, D.J., Adrian, R.J.: A particle image velocimetry system for microfluidics. Exp. Fluids **25**(4), 316–319 (1998)
Sato, Y., et al.: Solubilities and diffusion coefficients of carbon dioxide and nitrogen in polypropylene, high-density polyethylene, and polystyrene under high pressures and temperatures. Fluid Phase Equilib. **162**(1–2), 261–276 (1999)
Schmidt, M.A.: Wafer-to-wafer bonding for microstructure formation. Proc. IEEE **86**(8), 1575–1585 (1998)
Schwartz, G., Schaible, P.: Reactive ion etching of silicon. J. Vac. Sci. Technol. **16**(2), 410–413 (1979)
Seah, Y.F.S., Hu, H., Merten, C.A.: Microfluidic single-cell technology in immunology and antibody screening. Mol. Aspects Med. **59**, 47–61 (2017)
Seah, Y.F.S., Hu, H., Merten, C.A.: Microfluidic single-cell technology in immunology and antibody screening. Mol. Aspects Med. **59**, 47–61 (2018)
Sedaghat, M., Mohammadzadeh, O., Kord, S., Chatzis, I.: Heavy oil recovery using ASP flooding: a pore-level experimental study in fractured five-spot micromodels. Can. J. Chem. Eng. **94**(4), 779–791 (2016)
Sell, A., Fadaei, H., Kim, M., Sinton, D.: Measurement of CO_2 diffusivity for carbon sequestration: a microfluidic approach for reservoir-specific analysis. Environ. Sci. Technol. **47**(1), 71–78 (2013)
Shirota, H., Castner Jr., E.W.: Solvation in highly nonideal solutions: a study of aqueous 1-propanol using the coumarin 153 probe. J. Chem. Phys. **112**(5), 2367 (2000)
Shiu, P.P., Knopf, G.K., Ostojic, M., Nikumb, S.: Rapid fabrication of tooling for microfluidic devices via laser micromachining and hot embossing. J. Micromech. Microeng. **18**(2), 025012 (2008)
Sieben, V., Kharrat, A.M., Mostowfi, F.: Novel measurement of asphaltene content in oil using microfluidic technology. In: SPE Annual Technical Conference and Exhibition. Society of Petroleum Engineers, New Orleans (2013)
Silverio, V., de Freitas, S.C.: Microfabrication Techniques for Microfluidic Devices, Complex Fluid-Flows in Microfluidics, pp. 25–51. Springer, Berlin (2018)
Singh, R., et al.: Real rock-microfluidic flow cell: a test bed for real-time in situ analysis of flow, transport, and reaction in a subsurface reactive transport environment. J. Contam. Hydrol. **204**, 28–39 (2017)
Singh, R., et al.: Metabolism-induced $CaCO_3$ biomineralization during reactive transport in a micromodel: implications for porosity alteration. Environ. Sci. Technol. **49**(20), 12094–12104 (2015)
Sinton, D.: Energy: the microfluidic frontier. Lab Chip **14**(17), 3127–3134 (2014)
Song, W., de Haas, T.W., Fadaei, H., Sinton, D.: Chip-off-the-old-rock: the study of reservoir-relevant geological processes with real-rock micromodels. Lab Chip **14**(22), 4382–4390 (2014)
Song, W., Kovscek, A.R.: Functionalization of micromodels with kaolinite for investigation of low salinity oil-recovery processes. Lab Chip **15**(16), 3314–3325 (2015)
Song, W., Kovscek, A.R.: Direct visualization of pore-scale fines migration and formation damage during low-salinity waterflooding. J. Nat. Gas Sci. Eng. **34**, 1276–1283 (2016)
Stephan, K., et al.: Fast prototyping using a dry film photoresist: microfabrication of soft-lithography masters for microfluidic structures. J. Micromech. Microeng. **17**(10), N69 (2007)
Stevenson, J.T.M., Gundlach, A.M.: The application of photolithography to the fabrication of microcircuits. J. Phys. E: Sci. Instrum. **19**(9), 654 (1986)
Syed, A.H., et al.: A combined method for pore-scale optical and thermal characterization of SAGD. J. Petrol. Sci. Eng. **146**, 866–873 (2016)
Tan, S.H., Nguyen, N.-T., Chua, Y.C., Kang, T.G.: Oxygen plasma treatment for reducing hydrophobicity of a sealed polydimethylsiloxane microchannel. Biomicrofluidics **4**(3), 032204 (2010)
Tanino, Y., Zacarias-Hernandez, X., Christensen, M.: Oil/water displacement in microfluidic packed beds under weakly water-wetting conditions: competition between precursor film flow and piston-like displacement. Exp. Fluids **59**(2), 35 (2018)
Trietsch, S.J., Hankemeier, T., van der Linden, H.J.: Lab-on-a-chip technologies for massive parallel data generation in the life sciences: a review. Chemometr. Intell. Lab. Syst. **108**(1), 64–75 (2011)
Tropea, C., Yarin, A.L., Foss, J.F.: Springer Handbook of Experimental Fluid Mechanics. Springer, Berlin (2007)
Tsao, C.-W., DeVoe, D.L.: Bonding of thermoplastic polymer microfluidics. Microfluid. Nanofluid. **6**(1), 1–16 (2009)
Unsal, E., Broens, M., Armstrong, R.T.: Pore scale dynamics of microemulsion formation. Langmuir **32**(28), 7096–7108 (2016)
van der Helm, M.W., van der Meer, A.D., Eijkel, J.C., van den Berg, A., Segerink, L.I.: Microfluidic organ-on-chip technology for blood–brain barrier research. Tissue Barriers **4**(1), e1142493 (2016)
Verpoorte, E., De Rooij, N.F.: Microfluidics meets MEMS. Proc. IEEE **91**(6), 930–953 (2003)
Vladisavljević, G.T., Kobayashi, I., Nakajima, M.: Production of uniform droplets using membrane, microchannel and microfluidic emulsification devices. Microfluid. Nanofluid. **13**(1), 151–178 (2012)

Volpatti, L.R., Yetisen, A.K.: Commercialization of microfluidic devices. Trends Biotechnol. **32**(7), 347–350 (2014)
Wang, W., Chang, S., Gizzatov, A.: Toward reservoir-on-a-chip: fabricating reservoir micromodels by in situ growing calcium carbonate nanocrystals in microfluidic channels. ACS Appl. Mater. Interfaces **9**(34), 29380–29386 (2017)
Wang, X., Ding, B., Li, B.: Biomimetic electrospun nanofibrous structures for tissue engineering. Mater. Today **16**(6), 229–241 (2013a)
Wang, Y., et al.: Application of microfluidic technology for studying islet physiology and pathophysiology. Micro Nanosyst. **5**(3), 216–223 (2013b)
Wang, Y., et al.: Experimental study of crossover from capillary to viscous fingering for supercritical CO_2–water displacement in a homogeneous pore network. Environ. Sci. Technol. **47**(1), 212–218 (2013c)
Warkiani, M.E., et al.: Capturing and recovering of *Cryptosporidium parvum* oocysts with polymeric microfabricated filter. J. Membr. Sci. **369**(1), 560–568 (2011)
Warkiani, M.E., et al.: Slanted spiral microfluidics for the ultra-fast, label-free isolation of circulating tumor cells. Lab Chip **14**(1), 128–137 (2014a)
Warkiani, M.E., et al.: An ultra-high-throughput spiral microfluidic biochip for the enrichment of circulating tumor cells. Analyst **139**(13), 3245–3255 (2014b)
Webb, K.F., Teja, A.S.: Solubility and diffusion of carbon dioxide in polymers. Fluid Phase Equilib. **158–160**(1), 1029–1034 (1999)
Westerweel, J.: Fundamentals of digital particle image velocimetry. Meas. Sci. Technol. **8**(12), 1379 (1997)
White, C.M., et al.: Separation and capture of CO_2 from large stationary sources and sequestration in geological formations—coalbeds and deep saline aquifers separation and capture of CO_2 from large stationary sources and sequestration in geological formations—coalbeds. J. Air Waste Manag. Assoc. **53**(6), 645–715 (2003)
Whitesides, G.: The origins and the future of microfluidics. Nature **442**, 368–373 (2006a)
Whitesides, G.M.: The origins and the future of microfluidics. Nature **442**(7101), 368–373 (2006b)
Wiebe, R., Gaddy, V.L.: The solubility of carbon dioxide in water at various temperatures from 12° to 40° and at pressures to 500 atmospheres. Critical phenomena. J. Am. Chem. Soc. **62**(4), 815–817 (1940)
Wong, I., Ho, C.-M.: Surface molecular property modifications for poly(dimethylsiloxane)(PDMS) based microfluidic devices. Microfluid. Nanofluid. **7**(3), 291–306 (2009)
Wu, B., Kumar, A., Pamarthy, S.: High aspect ratio silicon etch: a review. J. Appl. Phys. **108**(5), 9 (2010)
Xu, B., et al.: High efficiency integration of three-dimensional functional microdevices inside a microfluidic chip by using femtosecond laser multifoci parallel microfabrication. Sci. Rep. **6**, 19989 (2016)
Xu, R., Li, R., Huang, F., Jiang, P.: Pore-scale visualization on a depressurization-induced CO_2 exsolution. Sci. Bull. **62**, 795–803 (2017)
Xu, W., Ok, J.T., Xiao, F., Neeves, K.B., Yin, X.: Effect of pore geometry and interfacial tension on water-oil displacement efficiency in oil-wet microfluidic porous media analogs. Phys. Fluids **26**(9), 093102 (2014)
Yadali Jamaloei, B., Kharrat, R.: Analysis of microscopic displacement mechanisms of dilute surfactant flooding in oil-wet and water-wet porous media. Transp. Porous Media **81**(1), 1 (2009)
Yang, S.Y., et al.: Single-file diffusion of protein drugs through cylindrical nanochannels. ACS Nano **4**(7), 3817–3822 (2010)
Yang, Y.-K., Yook, K.-J., Tae, J.: A rhodamine-based fluorescent and colorimetric chemodosimeter for the rapid detection of Hg2+ions in aqueous media. J. Am. Chem. Soc. **127**(48), 16760–16761 (2005)
Yaozhong, Z., Jea-Hyeoung, H., Likun, Z., Mark, A.S., Junghoon, Y.: Soft lithographic printing and transfer of photosensitive polymers: facile fabrication of free-standing structures and patterning fragile and unconventional substrates. J. Micromech. Microeng. **24**(11), 115019 (2014)
Yoon, H., Valocchi, A.J., Werth, C.J., Dewers, T.: Pore-scale simulation of mixing-induced calcium carbonate precipitation and dissolution in a microfluidic pore network. Water Resour. Res. **48**(2), W02524 (2012)
Yoon, J.-Y., Kim, B.: Lab-on-a-chip pathogen sensors for food safety. Sensors **12**(8), 10713–10741 (2012)
Zarikos, I.M., Hassanizadeh, S.M., van Oosterhout, L.M., van Oordt, W.: Manufacturing a Micro-model with Integrated Fibre Optic Pressure Sensors. Transport in Porous Media, New York (2018)
Zevi, Y., Dathe, A., McCarthy, J.F., Richards, B.K., Steenhuis, T.S.: Distribution of colloid particles onto interfaces in partially saturated sand. Environ. Sci. Technol. **39**(18), 7055–7064 (2005)
Zhang, C., Oostrom, M., Grate, J.W., Wietsma, T.W., Warner, M.G.: Liquid CO_2 displacement of water in a dual-permeability pore network micromodel. Environ. Sci. Technol. **45**(17), 7581–7588 (2011)
Zhang, J., Chen, K., Fan, Z.H.: Chapter one-circulating tumor cell isolation and analysis. In: Makowski, G.S. (ed.) Advances in Clinical Chemistry, pp. 1–31. Elsevier, Amsterdam (2016)
Zhang, Q., Karadimitriou, N.K., Hassanizadeh, S.M., Kleingeld, P.J., Imhof, A.: Study of colloids transport during two-phase flow using a novel polydimethylsiloxane micro-model. J. Colloid Interface Sci. **401**, 141–147 (2013)

Zhang, W., et al.: Liquid biopsy for cancer: circulating tumor cells, circulating free DNA or exosomes? Cell. Physiol. Biochem. **41**(2), 755–768 (2017)
Zhang, Y., Sanati-Nezhad, A., Hejazi, S.: Geo-material surface modification of microchips using layer-by-layer (LbL) assembly for subsurface energy and environmental applications. Lab Chip **18**(2), 285–295 (2018)
Zhao, B., MacMinn, C.W., Juanes, R.: Wettability control on multiphase flow in patterned microfluidics. Proc. Natl. Acad. Sci. **113**(37), 10251–10256 (2016)
Zheng, X., Mahabadi, N., Yun, T.S., Jang, J.: Effect of capillary and viscous force on CO_2 saturation and invasion pattern in the microfluidic chip. J. Geophys. Res. Solid Earth **122**(3), 1634–1647 (2017)
Zuo, L., Zhang, C., Falta, R.W., Benson, S.M.: Micromodel investigations of CO_2 exsolution from carbonated water in sedimentary rocks. Adv. Water Resour. **53**(6), 188–197 (2013)